ENSCO, INC.

5408A Port Royal Road
Springfield, Virginia 22151
Phone: (703) 321-9000

(12)

IMPROVED PROCEDURES FOR DETERMINING SEISMIC SOURCE DEPTHS FROM DEPTH PHASE INFORMATION

FINAL REPORT

Richard Houck
Edward Page

October 1, 1976
to September 30, 1977

Sponsored by:

Advanced Research Project Agency
ARPA Order No. 2551

APPROVED FOR PUBLIC RELEASE, DISTRIBUTION UNLIMITED

NOTICE OF DISCLAIMER

The views and conclusions contained in this document are those of the author and should not be interpreted as necessarily representing the official policies, either expressed or implied, of the Advanced Research Projects Agency, the Air Force Technical Applications Center, or the U.S. Government.

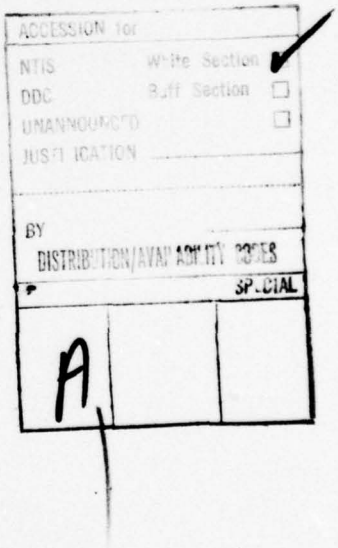

SECURITY CLASSIFICATION OF THIS PAGE (When Data Entered)

REPORT DOCUMENTATION PAGE

READ INSTRUCTIONS BEFORE COMPLETING FORM

1. REPORT NUMBER

2. GOVT ACCESSION NO.

3. RECIPIENT'S CATALOG NUMBER

4. TITLE (and Subtitle)

(6) Improved Procedures for Determining Seismic Source Depths from Depth Phase Information,

5. TYPE OF REPORT & PERIOD COVERED

(9) FINAL REPORT. 1 Oct 76-30 Sep 77

6. PERFORMING ORG. REPORT NUMBER

N/A

7. AUTHOR(s)

(10) Richard Houck, Edward Page

8. CONTRACT OR GRANT NUMBER(s)

F08606-77-C-0007

9. PERFORMING ORGANIZATION NAME AND ADDRESS

ENSCO, Inc.
5408A Port Royal Road
Springfield, VA 22151

10. PROGRAM ELEMENT, PROJECT, TASK AREA & WORK UNIT NUMBERS

VT/7710

11. CONTROLLING OFFICE NAME AND ADDRESS

DCASD
300 E. Joppa Road, Rm. 200
Towson, MD 21204

12. REPORT DATE

October 31, 1977

13. NUMBER OF PAGES

(11) 31 Oct 77

14. MONITORING AGENCY NAME & ADDRESS (if different from Controlling Office)

VELA Seismological Center
312 Montgomery Street
Alexandria, VA 22314

15. SECURITY CLASS. (of this report)

Unclassified (12) 75p.

15a. DECLASSIFICATION/DOWNGRADING SCHEDULE

16. DISTRIBUTION STATEMENT (of this Report)

(15) F08606-77-C-0007, VARPA Order-2551

APPROVED FOR PUBLIC RELEASE, DISTRIBUTION UNLIMITED

17. DISTRIBUTION STATEMENT (of the abstract entered in Block 20, if different from Report)

18. SUPPLEMENTARY NOTES

19. KEY WORDS (Continue on reverse side if necessary and identify by block number)

Seismic source depth, depth phase, nuclear discrimination, echo detection

20. ABSTRACT (Continue on reverse side if necessary and identify by block number)

The objective of this research has been to develop an improved technique for estimating the depths of seismic sources at teleseismic distances. Based on this depth estimate, deep events could immediately be classified as earthquakes and further discriminant analysis could be concentrated on the remaining shallow events.

(Continued)
next page

DD FORM 1 JAN 73 1473 EDITION OF 1 NOV 65 IS OBSOLETE

SECURITY CLASSIFICATION OF THIS PAGE (When Data Entered)

406 167 JOB

F-200.1473
ARMED SERVICES PROCUREMENT REGULATION

Work during this contract has been directed towards further improving and evaluating the automated depth determination procedure developed during three previous contracts. This procedure uses computed travel times to combine depth phase information associated with P, PP, PPP, and PcP arrivals recorded at a network of stations. The resulting depth estimate is better than those obtained by conventional methods, which do not make full use of all this depth phase information.

Significant program improvements implemented include a set of modifications which enhance the detection of depth phases, and a statistical technique for assessing the reliability of depth estimates. The depth determination procedure was evaluated by applying it to nine different events. Results of this analysis indicate that depth estimates with an error of ±3 km can be expected for events deeper than 10 km if sesimograms from at least five stations are available.

Finally, the depth determination procedure has been implemented at the Seismic Data Analysis Center (SDAC). This will permit the technique to be tested on a large base of events, for the purpose of thoroughly evaluating its place in the nuclear monitoring program.

SUBJECT: Improved Procedures for Determining Seismic Source Depths from Depth Phase Information

AFTAC Project No.	VELA T/7710
ARPA Order No.	2551
ARPA Program Code No.	6F10
Name of Contractor.	ENSCO, INC.
Contract No.	F08606-77-C-0007
Effective Date of Contract.	1 October 1976
Reporting Period.	1 October 1976 to 30 September 1977
Amount of Contract.	$89,923
Contract Expiration Date.	30 September 1977
Project Scientist.	Edward A. Page (703) 321-9000

TABLE OF CONTENTS

		PAGE
1.0	INTRODUCTION	1-1
2.0	PROGRAM DEVELOPMENT	2-1
	2.1 The Seismic Source Depth Determination Procedure	2-1
	2.2 Reduction of Spurious Depth Plot Peaks	2-3
	2.2.1 Cepstrum Processing	2-3
	2.2.2 Depth Plot Generation	2-6
	2.3 Calculation of Significance for Depth Plot Peaks	2-6
	2.4 Implementation at SDAC	2-11
3.0	ANALYSIS OF EVENTS	3-1
	3.1 Andreanof Islands Event	3-1
	3.2 Other Events	3-6
4.0	SUMMARY, CONCLUSIONS, AND RECOMMENDATIONS FOR FUTURE WORK	4-1
	4.1 Summary	4-1
	4.2 Conclusions	4-2
	4.3 Recommendations	4-3
APPENDIX -- Results of Event Analysis		A-1

1.0 INTRODUCTION

One of the most physically straightforward discriminants for underground explosions is source depth. If a sufficiently accurate method of estimating seismic source depth is available, those events deeper than possible for a man-made source can immediately be classified as earthquakes, and further analysis can be concentrated on the remaining shallow events. The basic objective of ENSCO's research in this area has been to develop a depth estimation technique that is sufficiently accurate and applicable enough for routine discriminant analysis.

At teleseismic distances, the most reliable information about the depth of an event is contained in the delay time between the depth phases and their corresponding primary phases. In practice, when an accurate depth estimate is desired, it is usually obtained from the pP-P delay time, determined by visually identifying the pP arrival. This technique works well when seismograms with clearly identifiable pP arrivals are available, but it is often not possible to pick pP unambiguously on any of the records at hand. An alternative approach is to use correlation techniques to estimate the pP-P time, but, when applied only to the first arrival portion of the seismogram, this method rarely produces better results than visual identification. Our basic approach has been to improve on these conventional depth determination methods by making more complete use of the information contained in the depth phases.

In the three previous contracts, the basic framework of an improved depth determination procedure was developed. The first contract (Project VT/4710) demonstrated that better estimates of p- and s- phase delay times could be obtained by applying cepstrum techniques to the entire P-wave coda, including

possible PP, PPP, and PcP arrivals and their corresponding depth phases. During the second contract (Project VT/5710), the cepstrum matched filter (CMF) algorithm was developed to simplify cepstrum interpretation by combining all the cepstrum peaks expected from correlations between p-, s-, and primary phases into a single peak. This contract also demonstrated the use of travel time information to correct for changes in the primary phase-to-depth phase delay times for later phases, enabling cepstrums computed from different parts of the seismogram to be constructively stacked. During the third contract (Project VT/6710), the use of travel time information was automated, resulting in a depth determination procedure that uses seismograms from a group of stations to produce plots of stacked cepstrum amplitude vs. depth. Ideally, these depth plots combine all the available depth phase information for an event into a single, easily interpretable display.

The basic objective of the present contract has been to improve on this depth determination technique and to apply it to a larger group of events. Along with many smaller program modifications, two major additions have been made to the depth determination procedure:

- A new cepstrum peak-picking algorithm that uses calculated s-phase delay times as well as p-phase times (replaces CMF).
- A statistical technique for estimating the significance of depth plot peaks.

The first of these new features is designed to do a better job of locating the desired cepstrum peaks, and the second is intended to simplify the interpretation of the final depth plots. Concurrent with this program development, nine new events were analyzed, with source depth estimates being made on eight of them.

Finally, the source depth analysis program has been implemented at the Seismic Data Analysis Center (SDAC). This is a totally rewritten program, and has several advantages over previous versions, including:

- easier access to data
- more flexibility in varying program parameters and analysis options
- more complete graphics (Calcomp plot) output

In this form, the depth determination procedure can be used for event analysis on a larger scale than has previously been practical, thus allowing the performance of the procedure to be more systematically analyzed.

This report describes the program development and event analysis work done during the past year. A brief outline of the depth determination procedure will be given, with more detailed accounts of the major new program features. Results from the nine events analyzed will be presented, along with their interpretations. Finally, the possibilities for further improvement and application of this procedure in the nuclear monitoring program will be discussed.

2.0 PROGRAM DEVELOPMENT

Basically, the program development done during this contract was directed towards simplifying the task of obtaining a source depth estimate. This has been accomplished by improving the depth determination procedure in three ways:

- Reducing spurious depth plot peaks
- Providing a more objective criterion for estimating the reliability of a given peak
- Allowing greater flexibility in changing key input parameters and analysis options

The following sections describe the particular program changes that have been made to obtain the desired improvement in each of these areas.

2.1 The Seismic Source Depth Determination Procedure

Before discussing particular program modifications, a brief description of the depth determination procedure is desirable; a more detailed treatment is given in the final report from the previous contract.

The basic components of this procedure are outlined in Figure 1. First, each seismogram to be processed is divided into a series of time windows of equal length, where the window length and the total amount of data to be used are user-input parameters. Next, a cepstrum is computed for each time window. Finally, the travel times for this station distance are computed for each trial depth and used to pick the cepstrum amplitudes to be accumulated into the appropriate individual phase depth plots.

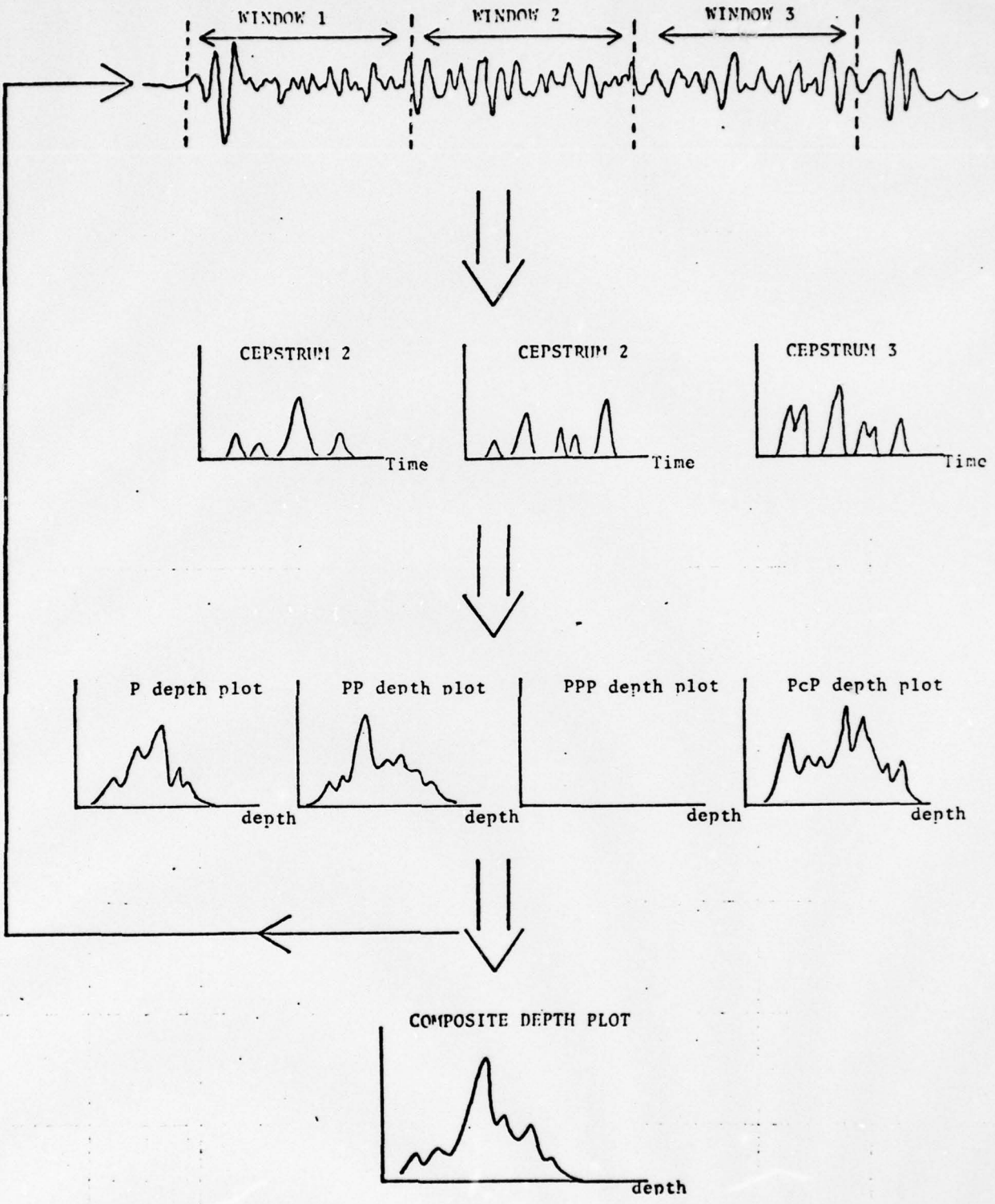

Figure 1. Depth Determination Procedure

The process is repeated for each station, resulting in four individual phase depth plots that contain depth information from all the seismograms. When every station has been processed, the individual phase plots are weighted according to the number of contributions and combined into a single composite depth plot, which contains all the depth information present in the whole set of seismograms. Ideally, the largest peak on the composite depth plot gives the best estimate of the source depth.

2.2 Reduction of Spurious Depth Plot Peaks

If all the assumptions implicit in the depth determination procedure were correct, the final depth plots would consist only of a single large peak at the true source depth, which includes information from two peaks arising from correlations between the p- and s- arrivals (difference peak) and between the primary and s- arrivals (second peak). Depth plots generated from real data, however, contain many additional peaks. The occurrence of these spurious peaks has been reduced by making modifications to both the cepstrum and depth plot processing algorithms.

2.2.1 Cepstrum Processing

Efforts were made to reduce false cepstrum peaks arising from two sources: inter-seismic phase correlations and source spectrum structure. The particular techniques used can be summarized:

- Removal of source spectrum structure
  - -- cosine taper of short lag part of cepstrum
  - -- spectrum whitening
- Reduction of inter-phase correlations
  - -- overlapping seismogram windows
  - -- arrival time controlled seismogram windows

The cosine taper resulted in a substantial improvement, and has been permanently incorporated into the depth determination procedure. The other techniques, however, require additional investigation to determine whether they can be useful.

Cosine Taper

Because of the large low frequency content of the source wavelet power spectrum, many high amplitude peaks tend to occur in the short lag part of the cepstrum, resulting in spurious depth plot peaks falling at shallow depths. One of these, corresponding to the first side lobe of the autocorrelation function, always occurs at a lag of 1.5 - 2.0 sec., producing a large depth plot peak near 7 km. This peak has been successfully eliminated by applying a cosine taper to the short lag part of each cepstrum. This technique was tested on four events: Illinois (Figure A-2), Andreanof Islands (Figure A-26, A-28), Turkey (Figure A-5), and Montana (Figure A-10), with clear improvement resulting in all cases. The success of this method for the Montana event, with an estimated depth of 13 km, demonstrates that the cosine taper does not degrade actual depth phase peaks, even for events with depths near 10 km.

Spectrum Whitening

A more general, and more effective, way of eliminating cepstrum peaks due to the structure of the source wavelet spectrum is to whiten the source spectrum. If the source wavelet had a flat amplitude spectrum, the cepstrum peaks resulting from depth phase correlations would be delta functions; the spurious peaks arising from low frequency modulation in the source spectrum would not be present. Several whitening techniques, including log whitening and inverse filtering, were tried in an effort to eliminate these peaks, but without success.

Overlapping Seismogram Windows

Spurious cepstrum peaks can also occur if arrivals from different primary phases (e.g., sP-PP, PPP-PP) fall into the same seismogram window. The first attempt at reducing these peaks involved computing cepstrums using overlapping time windows instead of non-overlapping windows. Although this does not prevent arrivals from different primary phases from falling within the same window, it does make it more likely that there will always be a time window that contains the complete set of primary, p-, and s- arrivals. On the small set of events analyzed, this technique failed to improve on the results obtained with non-overlapping windows.

Arrival Time-Controlled Seismogram Windows

The second approach to the inter-phase correlation problem used non-uniformly spaced, variable length time windows to guarantee that depth phases would always fall in the same window as their corresponding primary phases. For each primary phase, this method computes cepstrums from time windows starting at the expected arrival time for that phase, and extending far enough to include the corresponding s- arrival. Since the primary-to-s delay time increases with source depth, this method requires the simultaneous use of cepstrums computed from time windows of different lengths.

The arrival time controlled method also failed to produce the desired depth plot improvement. This technique, however, still seems like a good idea. Its lack of success may be due to inconsistent scaling between cepstrums computed from time windows of different lengths; further investigation in this area would probably be useful.

2.2.2 Depth Plot Generation

False depth plot peaks can also be introduced during the procedure that generates depth plots from cepstrums. To minimize this, several modifications have been made to the depth plot generation procedure; by far the most important of these is the use of calculated s-phase delay times in the cepstrum peak-picking algorithm. This has allowed the old CMF algorithm to be replaced by a much simpler one, and has eliminated one source of spurious peaks.

Basically, the availability of calculated s-delay times enables the program to locate difference and second peaks directly, instead of scanning over a range of T_{s-}/T_{p-} ratios as was done by CMF. For each trial depth and station, CMF used a 3-dimensional polynomial to calculate the expected delay time for the main peak, then scanned over a range of delay times for the difference and second peaks. This made it relatively easy to pick up high amplitude, spurious cepstrum peaks and miss the correct peaks entirely. With the inroduction of polynomial coefficients for s-phases, however, precalculated delay times can also be used for the difference and second peaks, thus reducing the chances of picking up a spurious peak.

2.3 Calculation of Significance for Depth Plot Peaks

Depth plots generated from real data will, in general, contain many peaks, and it is desirable to have some quantitative means of estimating whether any of these peaks indicate the true source depth. The distinguishing characteristic of cepstrum peaks that arise from depth phases is that their locations vary with station distance and seismic phase in the way expected by the cepstrum picking algorithm. Thus, these peaks will always contribute to the depth plots at the same depth, i.e, the source depth, for each cepstrum processed. Cepstrum peaks arising from other sources (interphase correlations, source spectrum structure, etc.) will not, in general,

vary between cepstrums in the way predicted by the p- and s-delay time calculations. These false cepstrum peaks, in contrast with the depth phase cepstrum peaks, will not stack when summed into the depth plot arrays. Consequently, the range of amplitudes in a depth plot that contains real depth information should be much larger than in a depth plot containing only false, non-depth phase peaks. Based on this difference, a quantitative technique for estimating the significance of depth plot peaks has been developed.

Basically, this technique consists of using the actual cepstrums for an event to generate a set of "random depth plots" containing no depth information. The statistical properties of these plots are then determined and compared with the real depth plots. If the real depth plots have peaks with amplitudes that are significantly higher than those predicted by the amplitude distribution in the random depth plots, then those peaks probably contain true depth information.

The first step in the significance level calculation is to generate a set of depth plots similar to those that would result from the cepstrums if they contained no depth phase information. This is done by choosing the cepstrum values that contribute to the depth plot at each depth using random delay times instead of the true delay times for the difference, main, and second peaks expected for that depth. Specifically, the contributon of a cepstrum $c(\tau)$ to this random depth plot $R(d)$ is determined by generating, for each depth d, three random numbers τ_1, τ_2, τ_3, uniformly distributed between 0 and the cepstrum window length. After arranging the numbers so that $\tau_1 \leq \tau_2 \leq \tau_3$, the value of the random depth plot at depth d is updated:

$$R(d) = R(d) + \begin{cases} c(\tau_1)+c(\tau_2)+c(\tau_3) & \text{if } 0.7 \max\,(c(\tau_1),c(\tau_3)) \leq c(\tau_2) \\ c(\tau_2) & \text{otherwise} \end{cases}$$

This is the same algorithm used to determine the contribution of a cepstrum $c(\tau)$ to the real depth plots, except that the use of random numbers prevents any true depth phase peaks present in $c(\tau)$ from contributing at the correct depth. In other words, the use of random delay times makes $c(\tau)$ look like it contains no depth phase information.

This procedure is repeated for each cepstrum, until all cepstrums have been processed and the final values for the random depth plot R(d) are obtained. This random depth plot can be viewed as a set of values of a random variable r with unknown probability distribution f(r); i.e.,

$$f(r) = \text{Probability} \quad R(d) = r$$

Note that r is not uniformly distributed, even though the random delay times are. This is because each r is a sum of cepstrum values, and each cepstrum $c(\tau)$ is a nonlinear function of the delay time.

The next step is to use R(d) to estimate f(r) and then to estimate the cumulative distribution function F(r) which will be used to obtain the desired significance level values. The details of this process are illustrated in Figure 2.

First, f(r) is estimated by dividing the amplitude axis on the random depth plot into intervals of width Δr and counting the number of points that fall in each interval. Then the estimated probability distribution is given by:

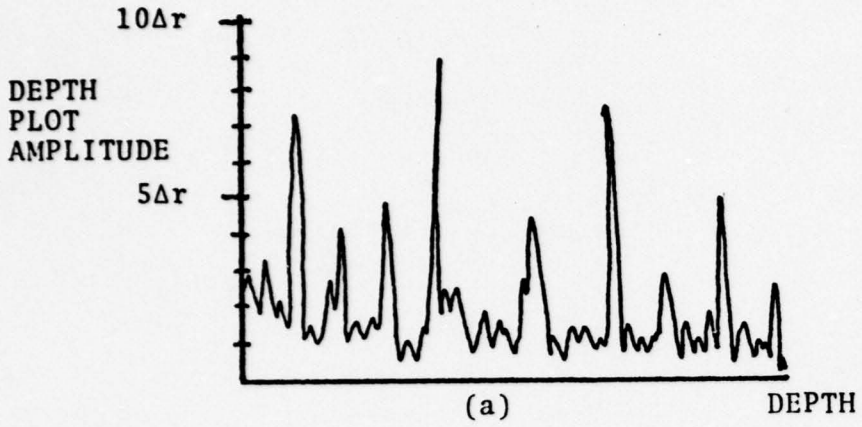

Random Depth Plot

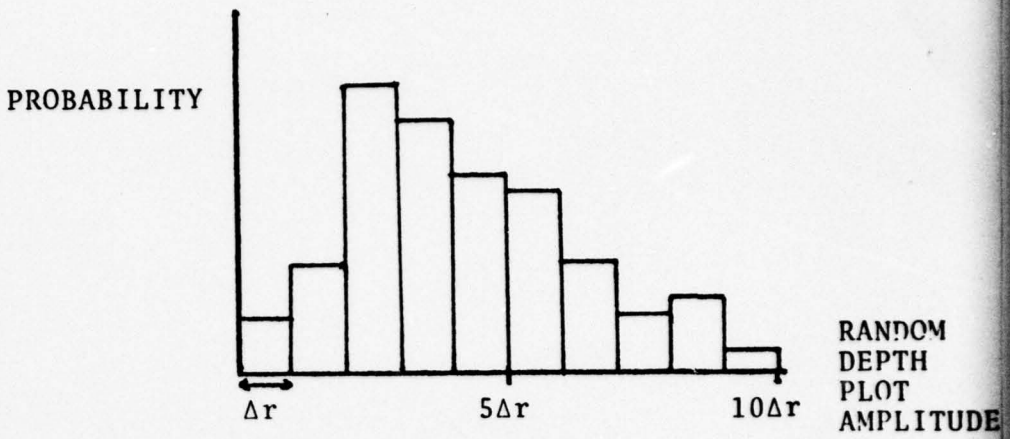

(b)

Estimated Probability Density f(r)

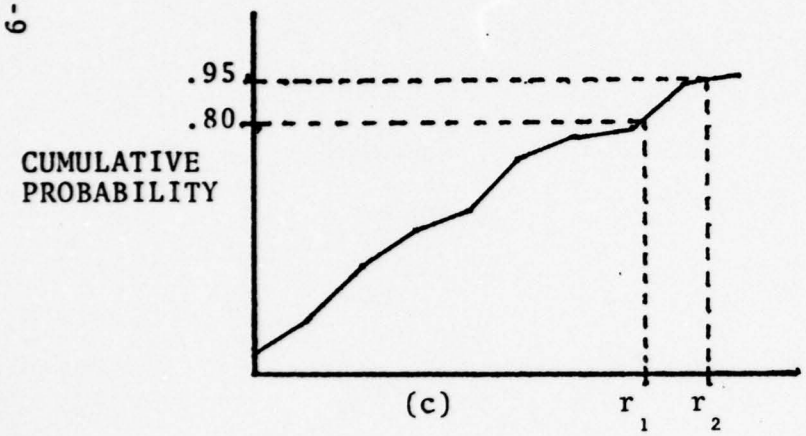

Cumulative Distribution F(r)

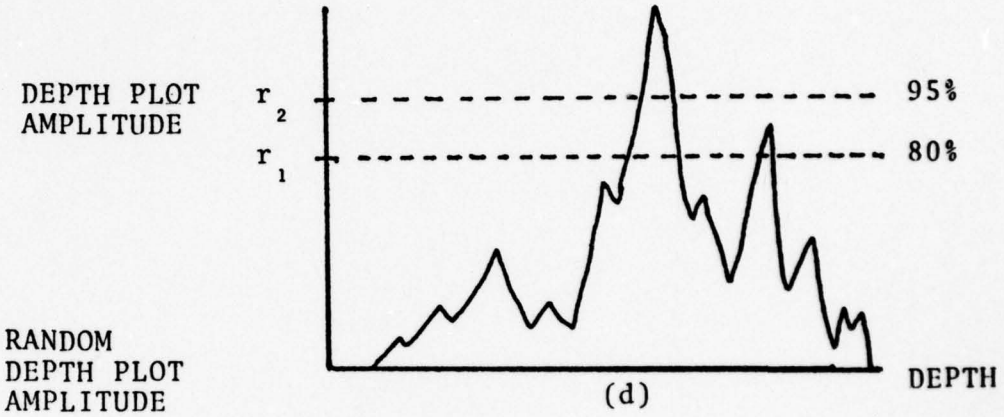

Final Depth Plot

Figure 2

Peak Significance Calculation

$$f(n\Delta r) = \frac{\text{no. of points with amplitudes in } ((n-1)\Delta r,\ n\Delta r)}{\text{total number of points}}$$

Next, this estimate of f(r), shown in Figure 2b, is used to find the cumulative distribution function F(r) by computing the sums

$$F(n\Delta r) = \sum_{i=1}^{n} f\ (i\Delta r)$$

Finally, F(r) is used to compute the significance levels as shown in Figure 2c. F(r) is the probability of getting a random depth plot point with a value <r, and the significance levels are given by the inverse of F(r). Specifically, the 80% and 95% significance levels are the depth plot values r_1 and r_2 that satisfy

$$F(r_1) = 0.80$$

$$F(r_2) = 0.95$$

These two values are marked on the final depth plot (Figure 2d), giving the analyst a quantitative criterion for estimating the validity of depth plot peaks. For example, if a depth plot has a peak amplitude above the 95% level (i.e., the amplitude that is greater than 95% of the points on the random depth plot), the peak (or peaks) containing these points are likely to contain real depth information. On the other hand, a peak that falls entirely below the 95% level could be a false one, even if it is the dominant peak on the depth plot, since 5% of the points computed using random delay times on the same cepstrums had a greater amplitude.

2.4 Implementation at SDAC

After most of the program development work had been completed, the source depth determination program was rewritten for implementation at SDAC. This version includes all the new features developed during this contract, and, in addition to allowing easier access to data, is characterized by increased flexibility in changing key input parameters and in obtaining different kinds of output. The basic purpose of this new version is to provide an efficient tool for performing source depth analysis on a large number of events.

The general flow of the SDAC depth determination program is shown in Figure 3. The program consists of two parts, enclosed by dashed lines in the figure, which can be executed either separately or together. The first part computes a set of cepstrums from the input seismogram data tape, and writes these cepstrums on an output tape. Control parameters, such as the total data length, cepstrum computation window length, and stations used, are input on data cards. Optional Calcomp plots of the seismograms may also be generated. The second part of the program reads the cepstrum file written by the first part and generates a set of depth plots. The control parameters used in producing the depth plots may either be the ones specified in the original run of the first step, or they may be new ones input to the second step on a set of override control cards. This override feature makes it possible to obtain sets of depth plots for different groups of stations, data lengths, window lengths, and other control parameters, without recomputing the cepstrums. Calcomp plots of individual cepstrums are also optionally available from the depth plot generation step. The various plots output by both steps are labelled with all identifying information and pertinent control parameters, and comprise a complete report of the depth analysis process for each event.

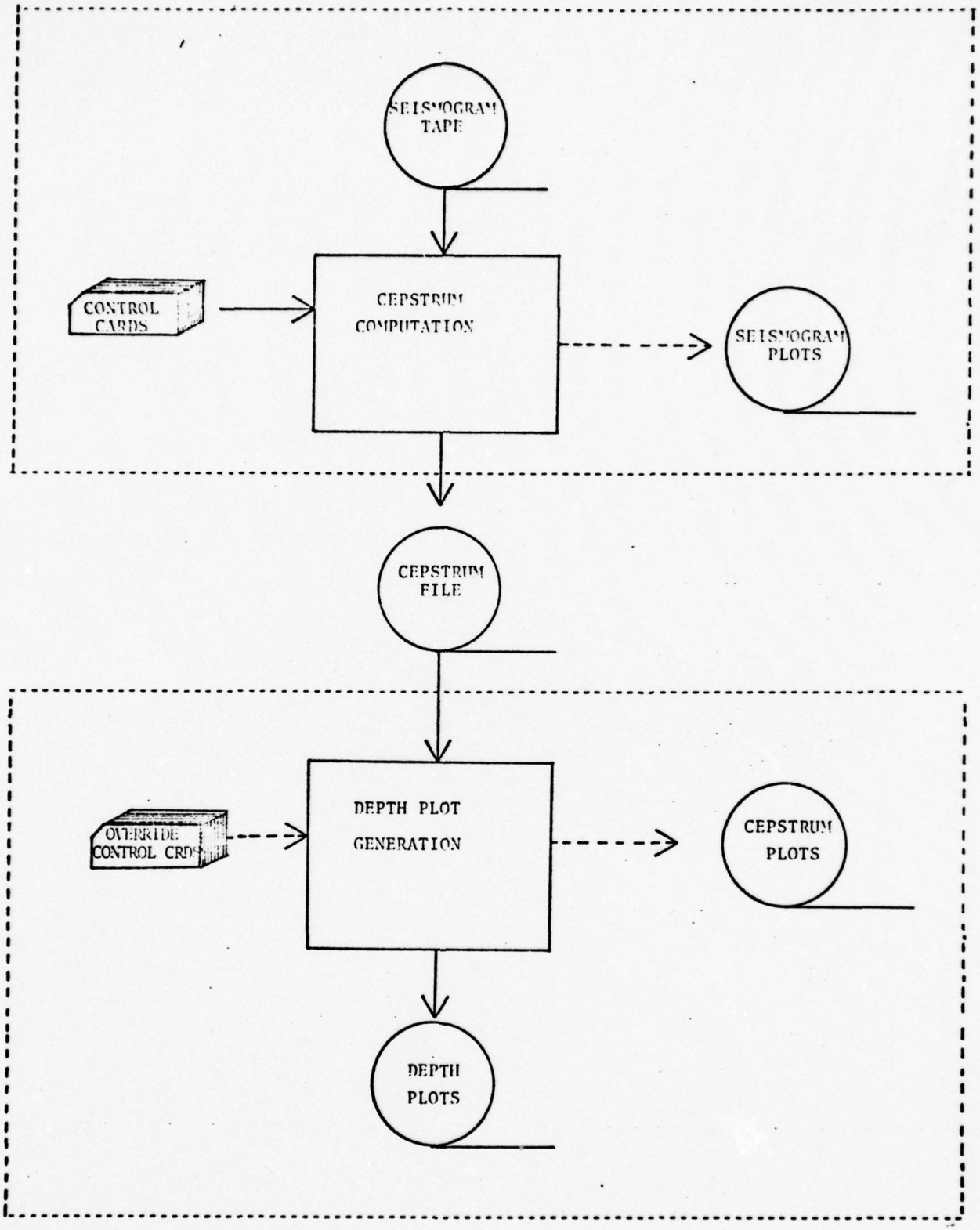

Figure 3. SDAC Depth Determination Program

3.0 ANALYSIS OF EVENTS

Nine events have been analyzed during this contract, with source depth estimates being made on all but one of them. Results of these analyses are summarized in Table 1; seismograms and key depth plots for each event can be found in the Appendix. A reliability grade has been listed in Table 1 for each event interpreted. This grade is a qualitative estimate of the reliability of the corresponding depth estimate, and is based on factors such as:

- appearance of depth plots
- number of stations processed
- seismogram signal-to-noise ratios
- significance level of peaks
- consistency of peaks among different stations and phases
- distribution of station distances

In this section, a detailed discussion of the interpretation of the Andreanof Islands event will be given. This event was chosen because of its complex interpretation, and because the large number of stations available allowed a more complete analysis to be performed. In addition, the interpretation of each of the remaining events will be briefly described.

3.1 Andreanof Islands Event

Data for the Andreanof Islands event consists of seismograms from 14 stations with Δ's ranging from 34° to 73°; these seismograms are shown in Figures A-21 and A-22. Because of the large number of stations available, the data could be divided into smaller groups of stations and each group processed separately. The resulting depth plots can then be used to

Table 1. Event Analysis Results

EVENT	NO. OF STATIONS	DEPTH	RELIA-BILITY	FIGURES
Illinois (11/9/68)	6	26 km	G	A-1, A-2
Turkey (3/27/75)	4	17 km	G	A-3 to A-5
Kuril (3/23/75)	3	39 km	F	A-6, A-7
Montana (6/30/75)	5	13 km	F	A-8 to A-10
Mojave Desert (6/1/75)	3	14 km	P	A-11, A-12
Idaho (3/28/75)	2	20 km	Q	A-13, A-14
Iran (3/7/75)	2	19 km	Q	A-15 to A-17
Kasmir (4/28/75)	2	----	--	A-18 to A-20
Andreanof Is. (11/22/65)	14	25 km	F	A-21 to A-38

RELIABILITY:

G = Good
F = Fair
P = Poor
V = Very Poor
Q = Questionable

check the behavior of individual peaks for different station groups, thus providing the interpreter with more information. This technique has proven to be quite useful, since the depth plots for this event contain three distinct peaks whose validity would be difficult to assess from only one large group of stations.

Seven different station groups were used in analyzing the Andreanof Islands event; the characteristics of these data sets are listed in Table 2. The resulting depth plots are shown in Figures A-23 through A-38. Each data set was run using the first 102.4 seconds of the seismograms, and depth plots were generated using window lengths of 25.6 and 51.2 seconds.

Four distinct peaks reappear consistently throughout all the depth plots, at depths of 7, 15, 25, and 42 km. The 7 km peak is an autocorrelation side lobe that can be eliminated by the cosine taper algorithm; Figures A-26 and A-28 (depth plots from Data Set 2 run with the cosine taper) show this clearly. The other three peaks, however, appear to represent real seismogram features.

Arrivals appear on many of the seismograms at delay times near 7 seconds and 10 seconds after P, suggesting that the 25 km peak should be interpreted as the main one, with the 42 km peak as the second peak and the 15 km peak as the difference peak. Estimates of the "average" delay times corresponding to these peaks show that the 15 km peak, with a delay time of about 4.5 seconds, does correspond to the difference peak between the 25 km (7.1 seconds) and 42 km (11.7 seconds) peaks. However, the 42 km peak is more than 1 second later than the expected sP time for a 25 km source depth. This anomalously late arrival explains why the cepstrum picking algorithm failed to sum the difference and second peak amplitudes into the main peak.

Table 2. Andreanof Islands Event Data Sets

DATA SET NO.	DESCRIPTION
1	5 stations, distributed over entire available range of Δ's
2	10 stations, distributed over entire available range of Δ's
3	4 stations, Δ's within 5° of Δ=39° (close range Δ's)
4	6 stations, Δ's within 5° of Δ=48° (middle range Δ's)
5	4 stations, Δ's within 5° of Δ=61° (long range Δ's)
6	8 stations, arrival visible 7 sec after P.
7	5 stations, arrival visible 10 sec after P

The long s delay time is most straightforwardly explained as a sP arrival from a source region with abnormally slow S velocities. An alternative interpretation is that there are two good reflectors, such as water bottom and water surface, above the source, with a two-way travel time of about 4.5 seconds between the two boundaries. Then, the 25 km peak would be the result of an echo off the deeper reflector, and the 42 km peak would come from an echo off the shallower reflector.

Thus, the interpretation of this event can be summarized:

- The 15 km peak is a difference peak arising from the 25 km and 42 km peaks.
- Two interpretations are possible for the 25 km and 42 km peaks:
  1. The 25 km peak represents a pP arrival (and thus the true source depth), and the 42 km peak represents a slow sP arrival.
  2. There are two reflectors above the source, with the 25 km peak coming from an echo off the deeper one, and the 42 km peak from an echo off the shallower one.

This event is a good one for illustrating how many factors can be involved in obtaining a depth estimate. Seismogram plots, delay time information, and depth plots from several different station groups have all been used in the interpretation of this event. All this information should be easily available to an analyst doing routine depth determinations, and each of these features is either included in or planned for the depth determination program implemented at SDAC.

3.2 Other Events

Illinois Event

The two events that were easiest to interpret and yielded the most reliable depths were Illinois and Turkey. Both events are characterized by depth plots with a single dominant peak, well above the 95% level, and have seismograms with good signal-to-noise ratios from an adequate number of stations. Several of the seismograms from these two events show clear pP arrivals with delay times that agree with the estimated source depths.

The Illinois event (Figures A-1 and A-2) is the same one analyzed during the previous contract. The six stations processed have source-to-receiver distances covering a range sufficient to produce significant moveout in depth phase delay times. P, PP, and PPP arrivals are present in at least some of the seismograms, and the resulting individual phase depth plots all have their highest amplitude peaks near 26 km. The depth plot shown in Figure A-2 is the composite plot obtained using the cosine taper program version, and is the most current result on this event. The high amplitudes that occur between 10-15 km are probably due to a combination of difference peaks and source spectrum structure.

Turkey Event

The Turkey event (Figures A-3 through A-5) has fewer stations and a smaller range of station distances than Illinois, but the resulting depth plots lack the spurious shallow peaks present in Illinois. Comparison of depth plots without and with the cosine taper shows how this technique reduces the peaks at depths less than 10 km.

Kuril Event

The Andreanof Islands, Kuril, and Montana events fall into the next reliability grade below Illinois and Turkey. The Kuril event (Figures A-6 and A-7) has a well-defined depth plot peak, and the three seismograms that were processed are all of good quality; the reliability for this event was downgraded mainly because so few stations were available. Significance levels are not present on the depth plot for this event, since it was run before the significance level algorithm was implemented. pP and sP arrivals are visible on the seismogram from WH2YK, at delay times that correspond to the estimated 39 km depth.

Montana Event

The Montana event (Figures A-8 through A-10) has a main depth plot peak that is not as clear-cut as those on the previously discussed events, and its significance level is somewhat lower. However, the fact that five stations were used in the processing lends more credibility to this peak. Although some of the seismograms are of poor quality, the use of all five stations was still found to produce the most interpretable result. This event has clearly been helped by the introduction of the cosine taper, in spite of its shallow focal depth.

Mojave Desert Event

The depth estimate for the Mojave Desert event (Figures A-11 and A-12) is not as reliable as the Kuril and Montana events, even though the composite depth plot shows a good peak, well above the 95% level. This event was downgraded for three reasons. First, the significance level algorithm is of questionable validity when applied to such a small number of stations. Second, the three station distances are clustered around 25°, so there is practically no station moveout in the

depth phase delay times. Third, only two of the three seismograms have a good signal-to-noise ratio. Thus, although the estimated depth of 14 km is a valid one, it is not as reliable as the depth plot suggests.

Idaho Event

The Idaho and Iran events were analyzed using only two stations each, and the resulting depth plots are cluttered and ambiguous. Depth estimates have been made for both of these events, but their reliability is questionable. The Idaho event (Figures A-13 and A-14) has no single, dominant peak on the composite depth plot, although the correct depth probably lies somewhere in the high amplitude region between 16-27 km. Three stations were available for this event, but only two were used in the final depth plot; including the WH2YK seismogram was found to deteriorate the depth plots.

Iran Event

For the Iran event (Figures A-5 to A-17), conflicting depth plots were obtained when two different window lengths were used. Interpretation is hampered by the large (>90°) distances for both stations, resulting in only P arrivals being present, and by the fact that the significance level algorithm is meaningless for such a small amount of data. The 19 km peak on the 25.6 second depth plot has been picked as the depth estimate, since some evidence of this peak can also be seen on the 12.8 second plot.

Kasmir Event

No depth estimate has been make for the Kasmir event (Figures A-18 through A-20). This event is similar to the Iran event, but the 17 km peak that appears to be the best depth estimate on the 12.8 second depth plot is not present at all on the 25.6 second plot. Both depth plots contain a lot of shallow

depth noise, and their interpretability may have been improved if the cosine taper algorithm had been available.

4.0 SUMMARY, CONCLUSIONS, AND RECOMMENDATIONS FOR FUTURE WORK

4.1 SUMMARY

Two major additions have been made to the source depth determination procedure during this contract: the calculation and use of s-phase travel times in the cepstrum picking algorithm, and a statistical technique for determining the significance of depth plot estimates. Several techniques for reducing spurious cepstrum peaks were also investigated, and one of them, found to be very useful for reducing short delay time peaks, has been permanently implemented. Finally, a totally re-written version of the depth determination program has been implemented at SDAC, allowing this method to be used for event analysis on a larger scale than has previously been practical.

A total of nine new events have been analyzed with depth estimates being obtained on eight of them. Results are summarized in Table 1 (p.3-2). Two of these events had depth plots with a single dominant peak, well above the 95% significance level, and had seismograms with good signal-to-noise ratios from four or more stations, and the resulting depth estimates were classified as having good reliability. Three events had either fewer stations or more ambiguous depth plots than the first two, and their depth estimates were classified as fair. One event had only three seismograms, with one of them being very noisy, and had a station distribution that resulted in very little moveout in the depth phase delay times, so its depth estimate was classified as poor. Two more events were classified as questionable because of very ambiguous depth plots and small number of stations. Finally, no depth estimate could be made on one event.

4.2 CONCLUSIONS

The results of the two principal program changes made during this work were investigated while processing the nine events. The use of calculated s-phase delay times was found to generally improve the quality of the depth plots. This improvement, however, is not large, and is probably more due to elimination of the noise introduced by the time scan in the old CMF algorithm than to better detection of s-phases. The availability of s-phase delay times greatly simplifies the depth plot generation process, and does do a better job of finding s-phases when they are present, so it is a useful addition to the program. The significance level algorithm was found to usually do a good job of estimating the significance of depth plot peaks, but it did not appear to work well when only small amounts of data are available. This is to be expected in view of the statistical nature of this technique.

The results from event analysis also provided new information on the accuracy of depth estimates. Basically, these events showed that the errors involved in this depth determination procedure are of two kinds: peak detection errors and peak precision errors. Peak detection error is concerned with whether the depth determination procedure has successfully detected depth phases and displayed the depth information as an interpretable depth plot peak; i.e., whether the analyst is able to choose the correct depth plot peak for his depth estimate. The significance level algorithm is designed to reduce this kind of error by providing a quantitative criterion for deciding whether a depth plot peak has come from depth phases or noise. Ideally, peak detection error should be quantified as the probability of finding the correct depth plot peak, but this requires a large data base of events with independently known depths. Thus, a qualitative estimate of the peak detection probability, such as the reliability grades

given in Table 1, must be used. Based on the events listed in Table 1, the probability of successful peak detection is "good" for events with at least five good quality seismograms available.

The second kind of error, peak precision error, is the numerical error in the estimated depth, assuming the correct depth plot peak has been picked. This error depends on factors such as depth phase delay time errors, seismogram spectra, and properties of processing procedures such as cepstrum filtering and power spectrum tapering. For the set of events analyzed, peak precision error has been estimated at ±3 km.

Combining these two kinds of errors, the events processed to date indicate that, for events deeper than 10 km, the depth determination procedure will have a "good" probability of estimating the source depth to ±3 km if at least five stations are available.

4.3 RECOMMENDATIONS

Some additional testing and program development is necessary before this technique will be ready for routine use in the nuclear monitoring program. First, the depth determination procedure should be applied to a large base of events. This will more firmly establish the applicability of the method in a wide range of situations, and will permit its performance to be investigated as a function of source parameters, station distribution, and sesimogram characteristics. This large scale testing is the function of the program version that has been implemented at SDAC. Next, the possibilities for further program development discovered during this contract need to be investigated. These include additional work on the significance level algorithm and the use of phase information in the depth phase detection procedure.

Finally, the analysis of the Andreanof Islands event has shown that the depth determination procedure should eventually be put in a fully interactive form. Routine processing of seismic events by an analyst requires easy access and display of information such as sesimograms, travel times, and results from individual stations, as well as the capability of obtaining rapid output using new program parameters. All these features will be available if the depth determination procedure is implemented on an interactive graphics system.

APPENDIX

RESULTS OF EVENT ANALYSIS

Figure A1

Illinois Event Seismograms

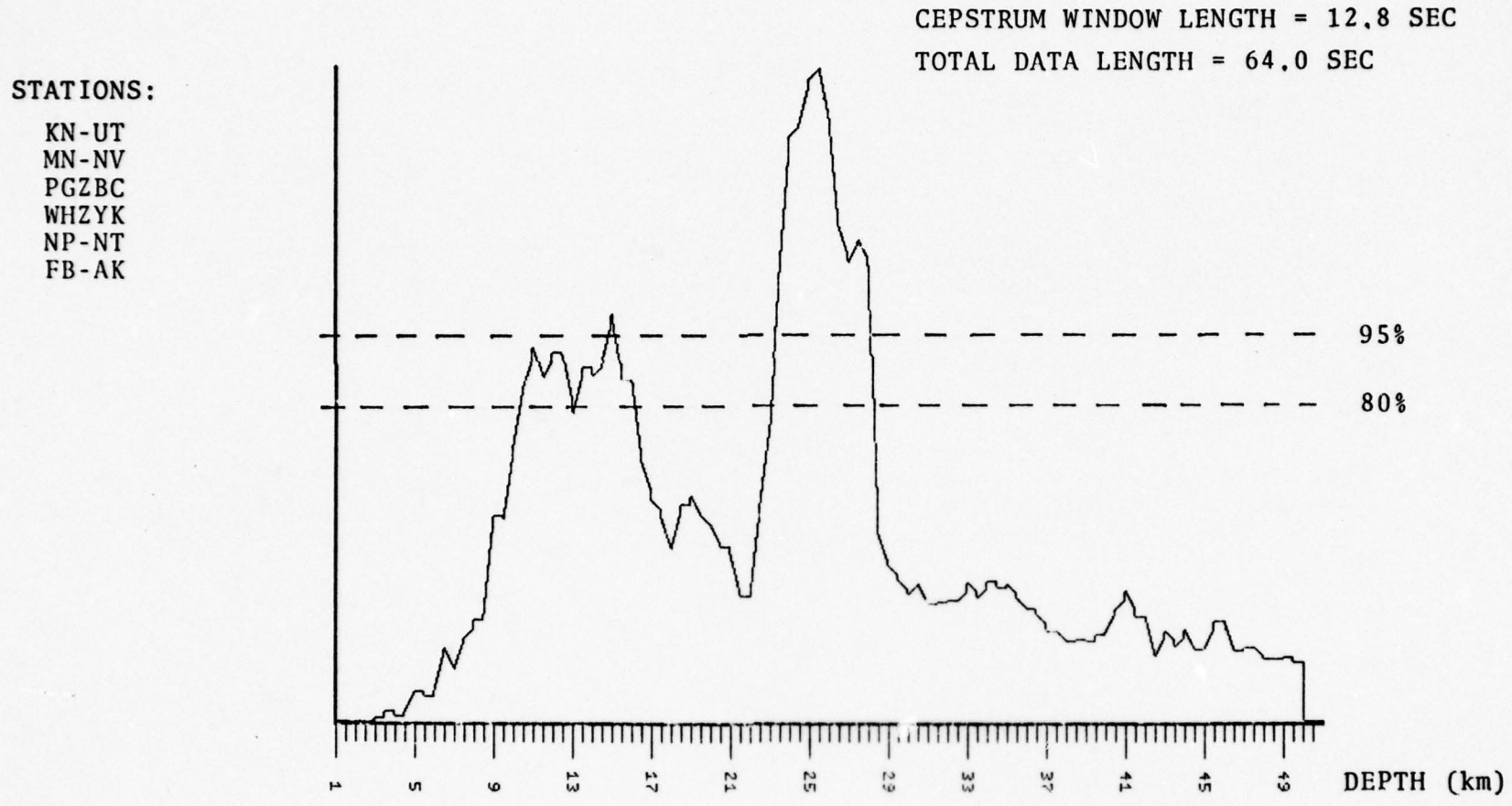

Figure A2

Illinois Event Composite Depth Plot, Cosine Taper

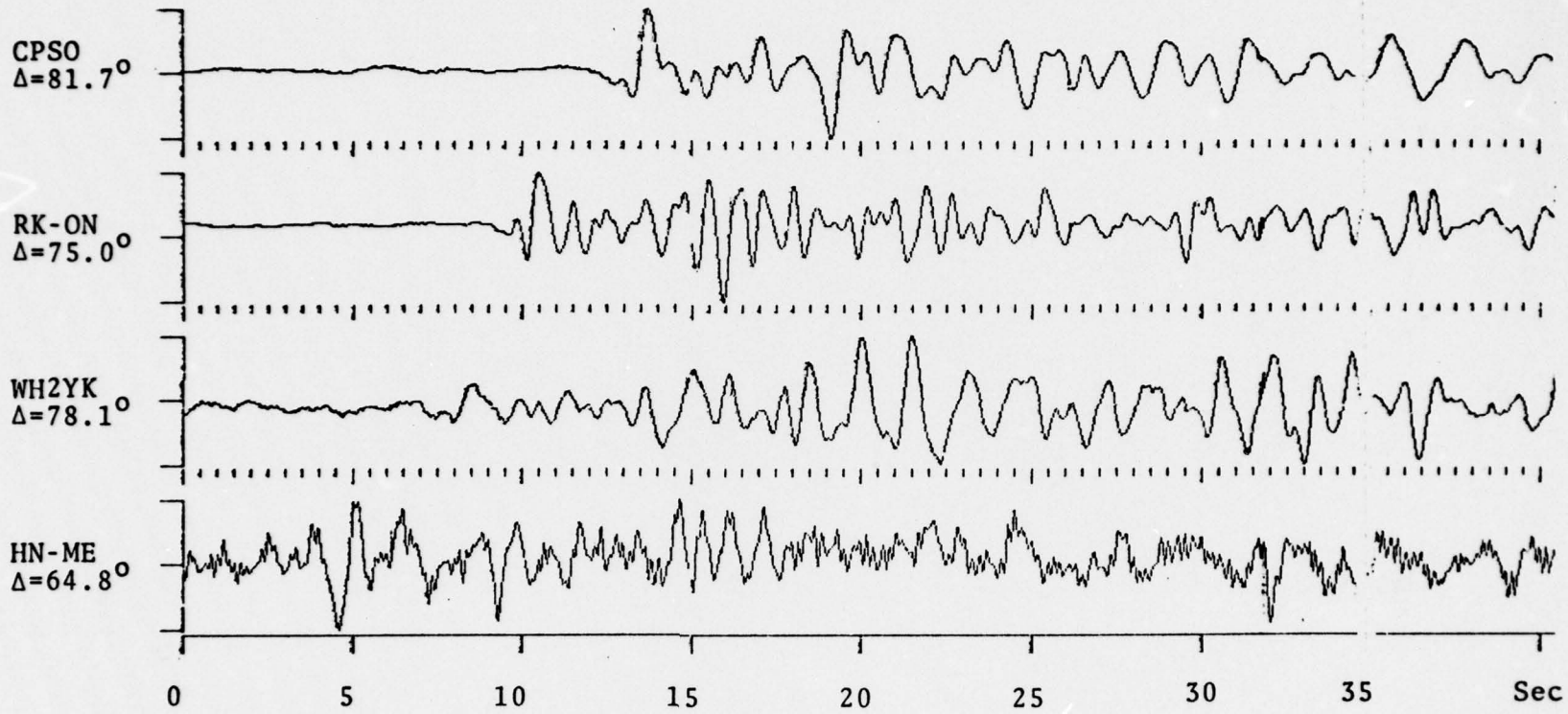

Figure A3

Turkey Event (3/27/75) Seismograms

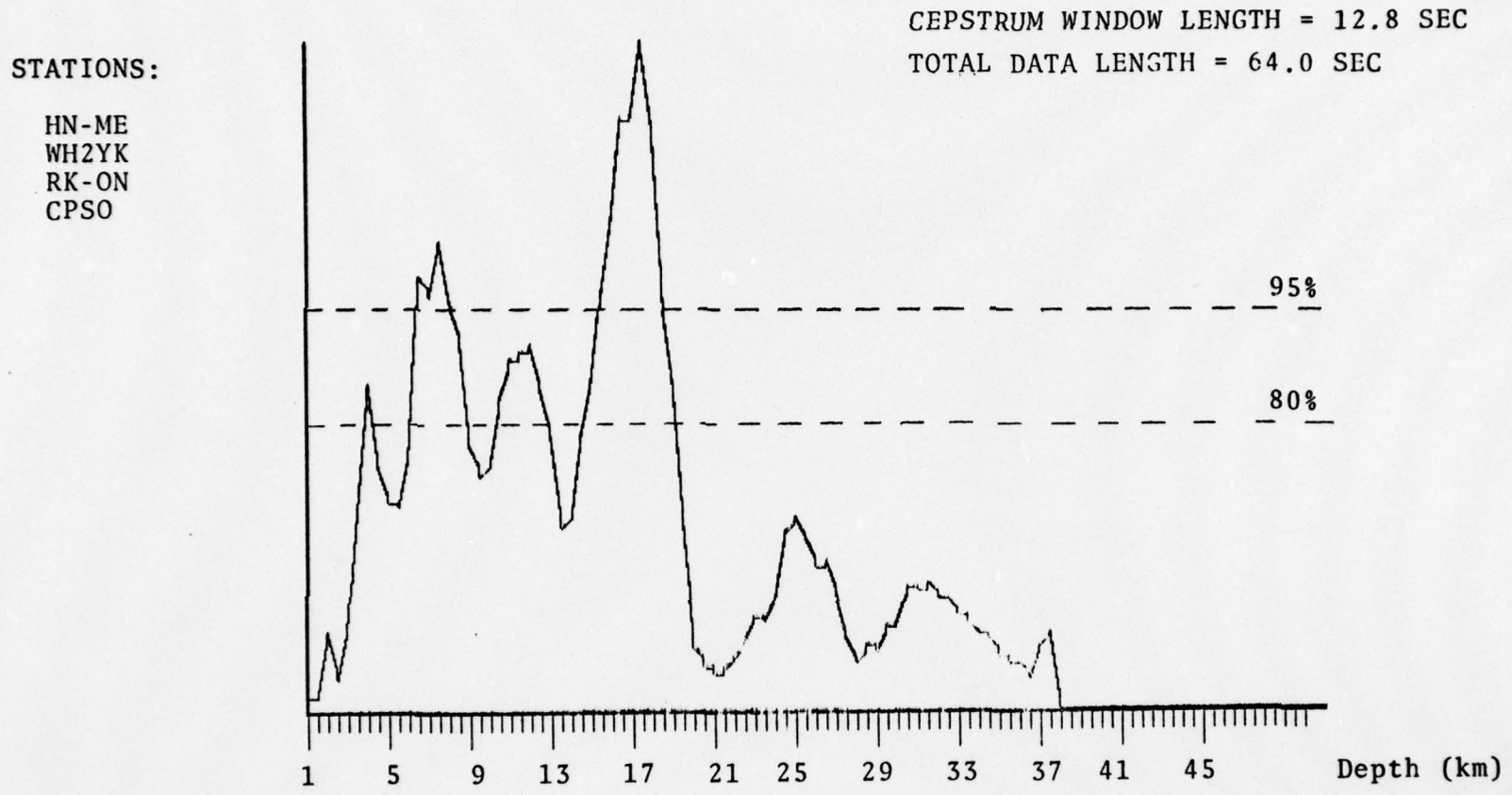

Figure A4

Turkey Event (3/27/75), Composite Depth Plot

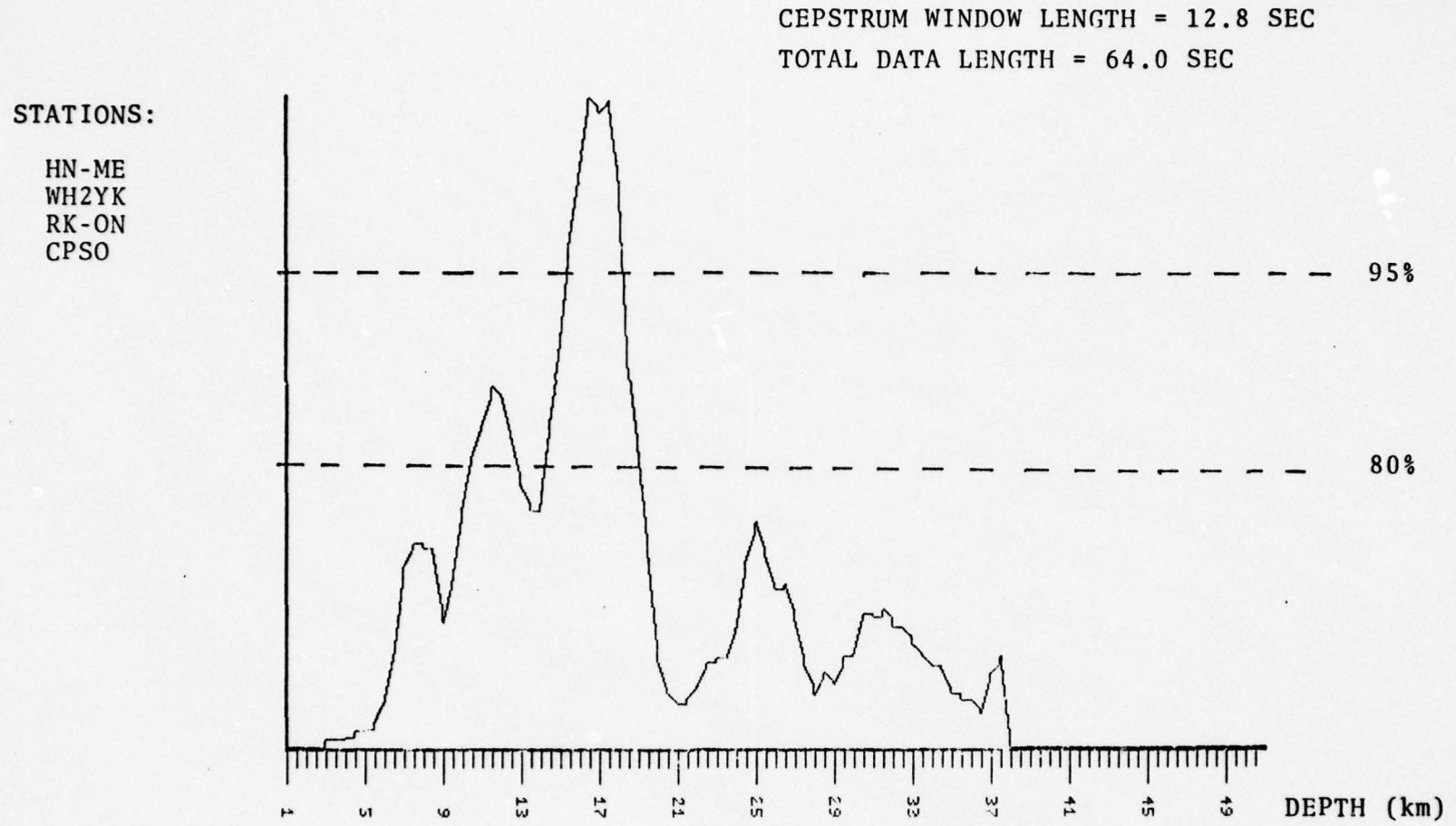

Figure A5

Turkey Event Composite Depth Plot, Cosine Taper

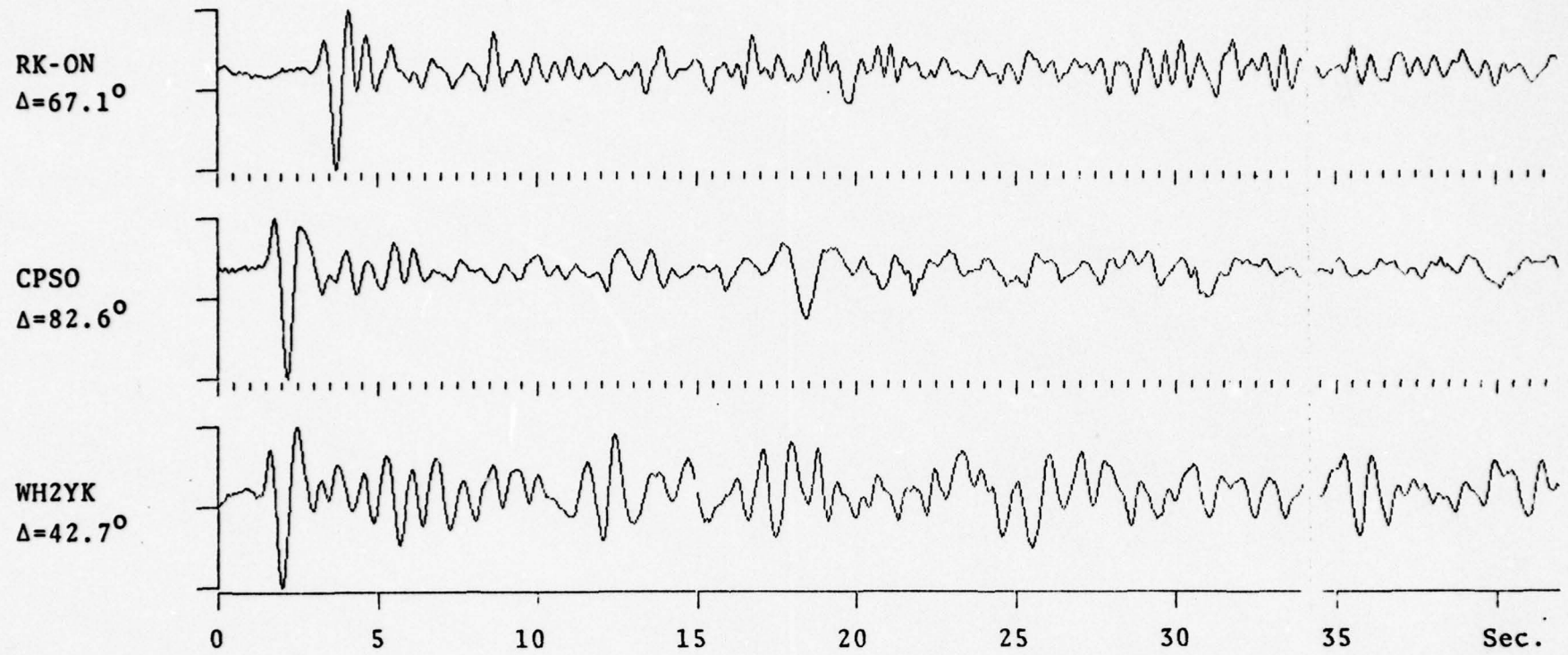

Figure A6

Kuril Event (3/23/75) Seismograms

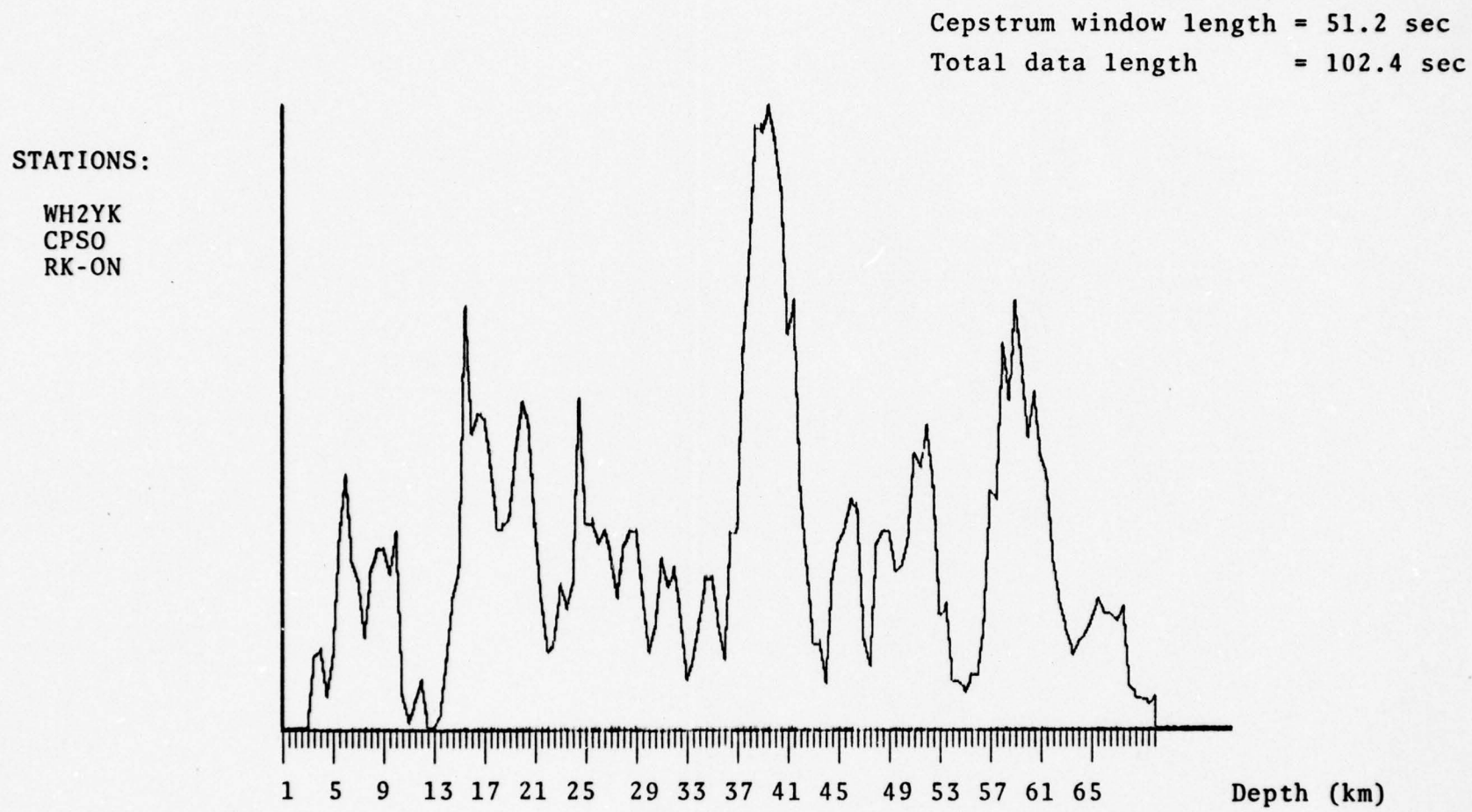

Figure A7

Composite Depth Plot, Kuril Event (3/23/75)

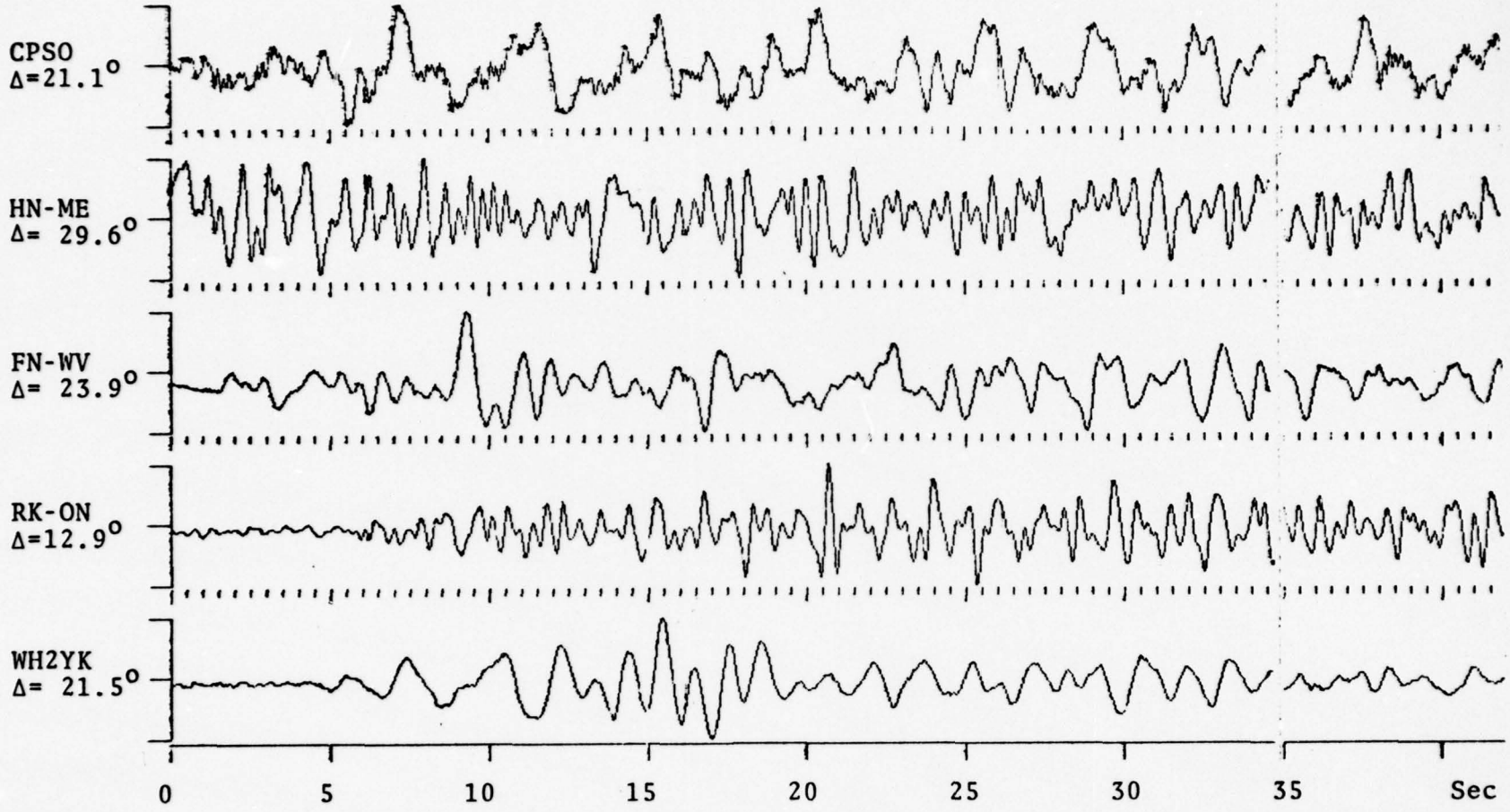

Figure A8

Montana Event (6/30/75) Seismograms

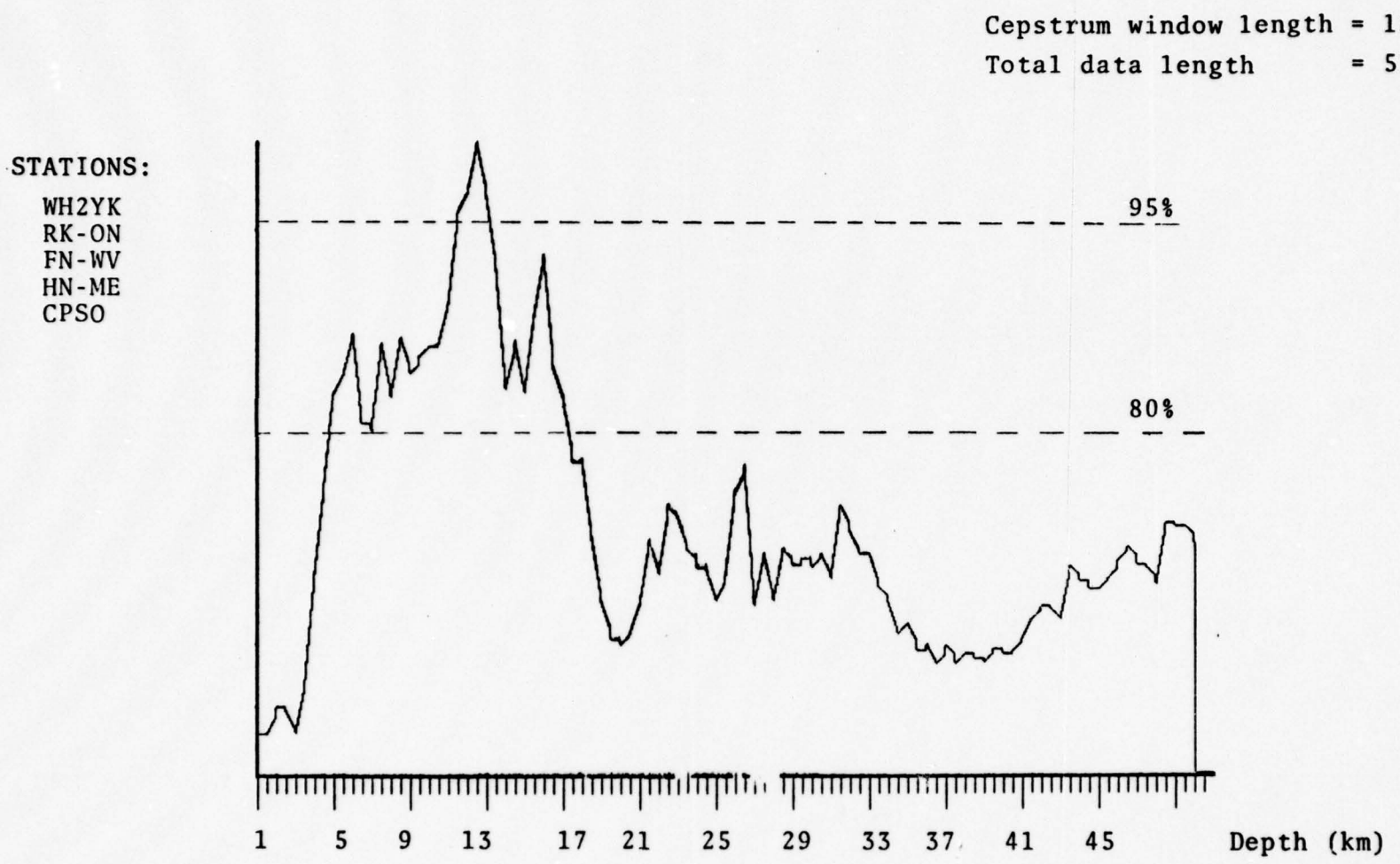

Figure A9

Montana Event (6/30/75), Composite Depth Plot

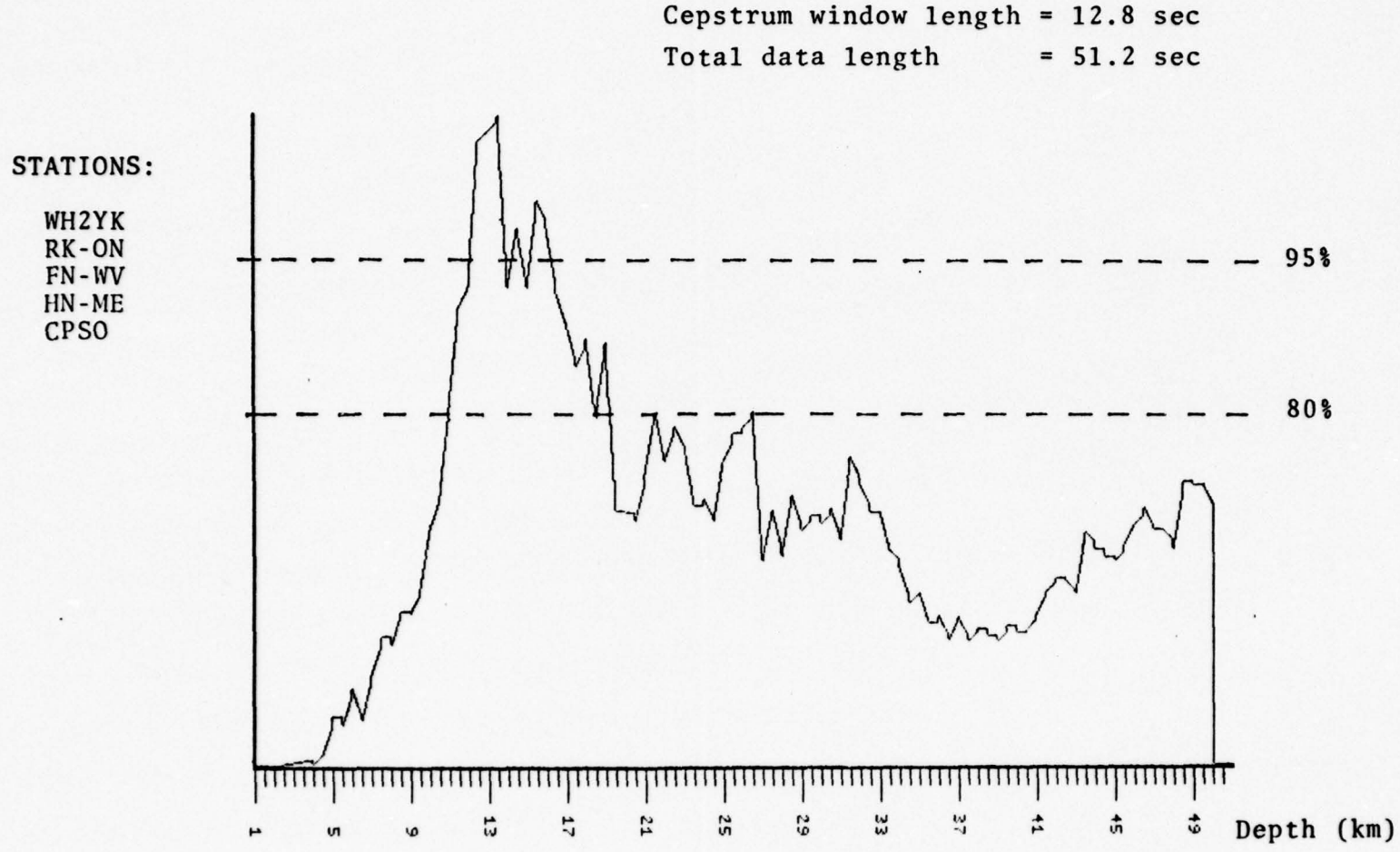

Figure A10

Montana Event (6/30/75), Composite Depth Plot, Cosine Taper

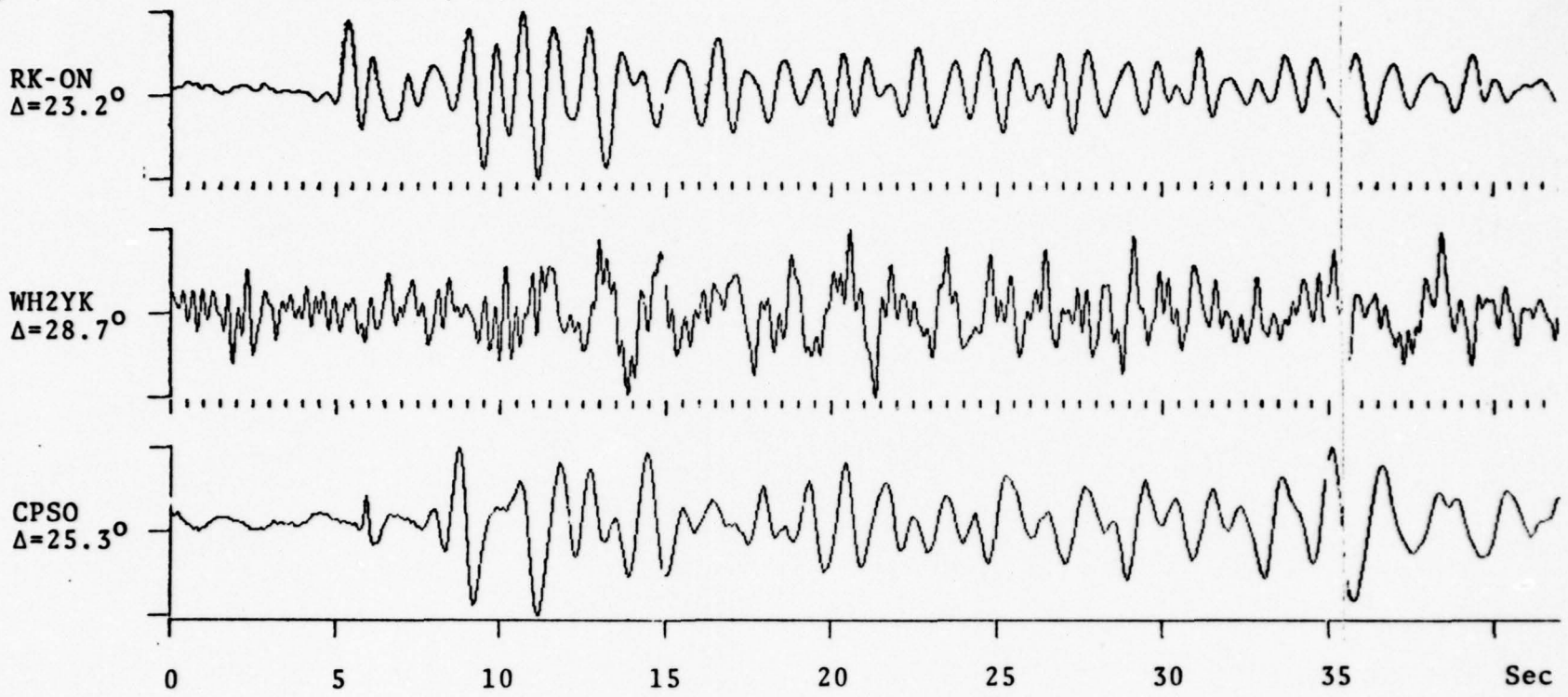

Figure A11

Mojave Desert Event (6/1/75), Seismograms

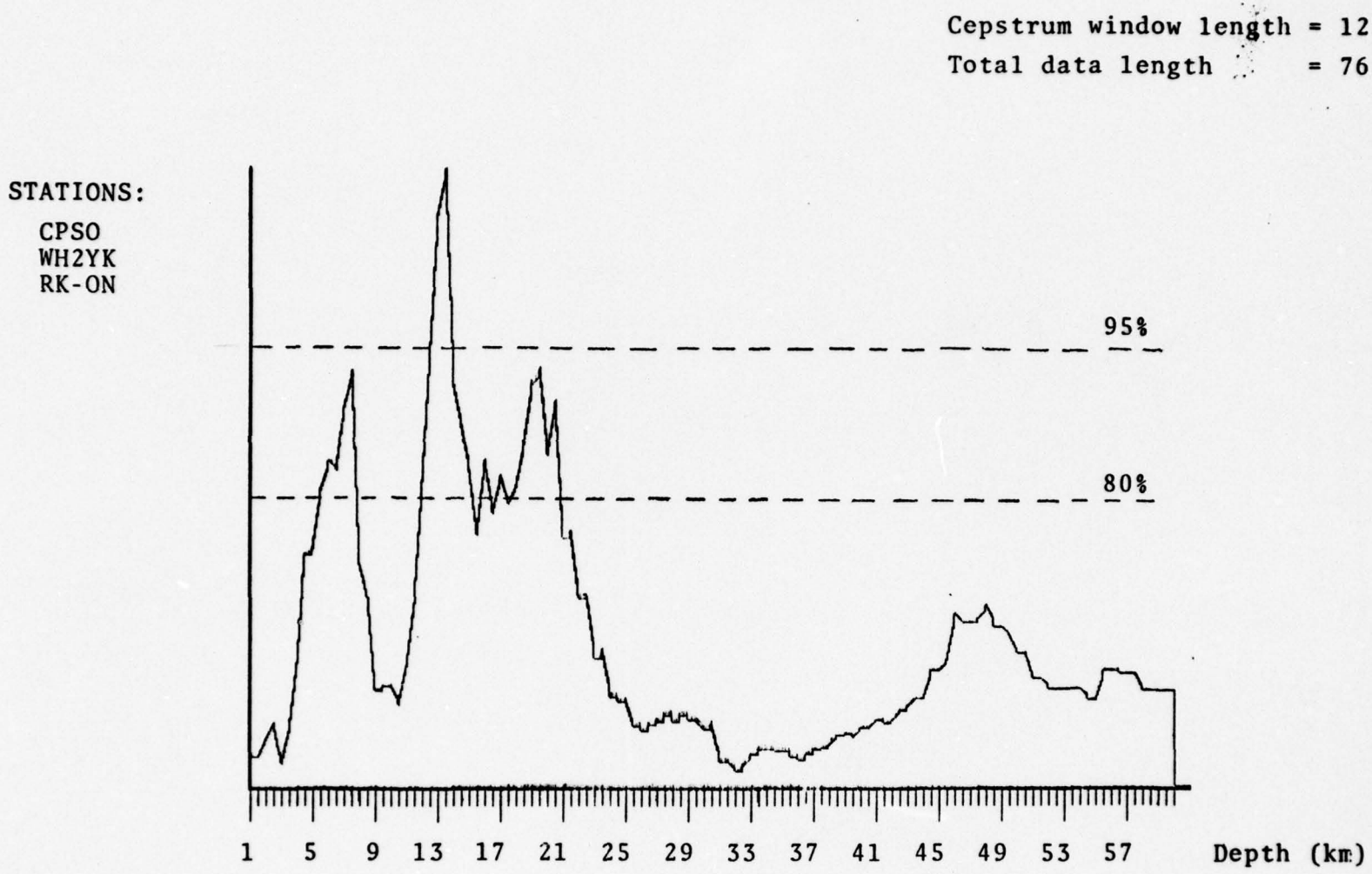

Figure A12

Mojave Desert Event (6/1/75), Composite Depth Plot

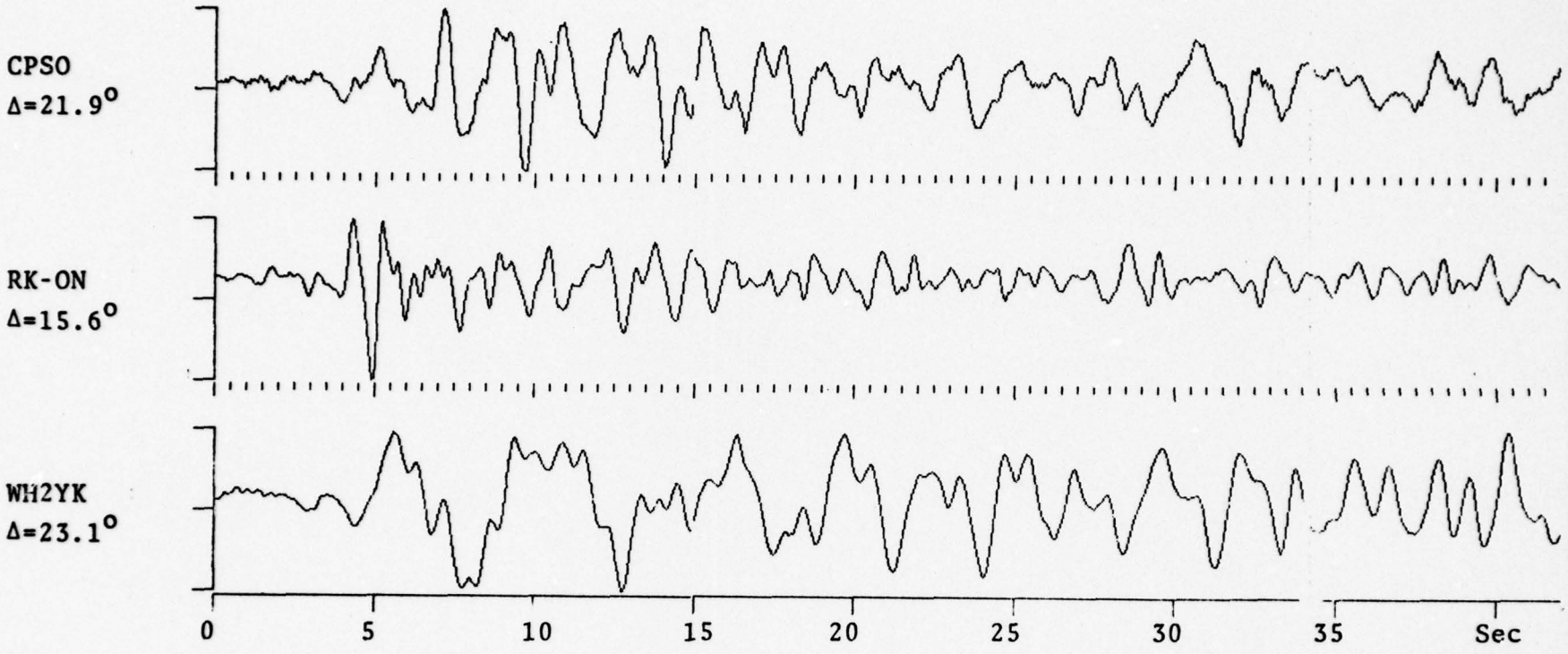

Figure A13

Idaho Event (3/28/75) Seismograms

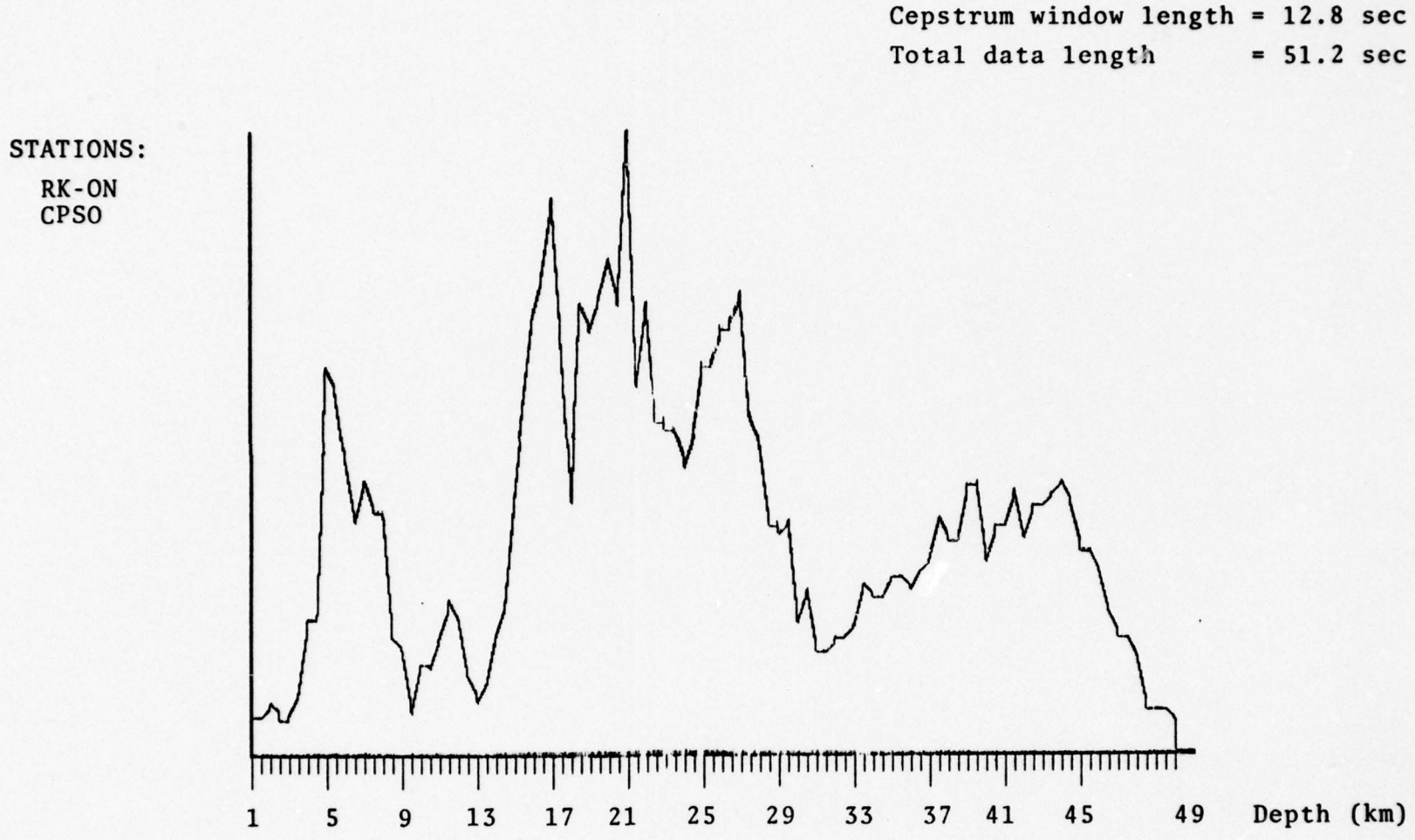

Figure A14

Composite Depth Plot, Idaho Event (3/28/75)

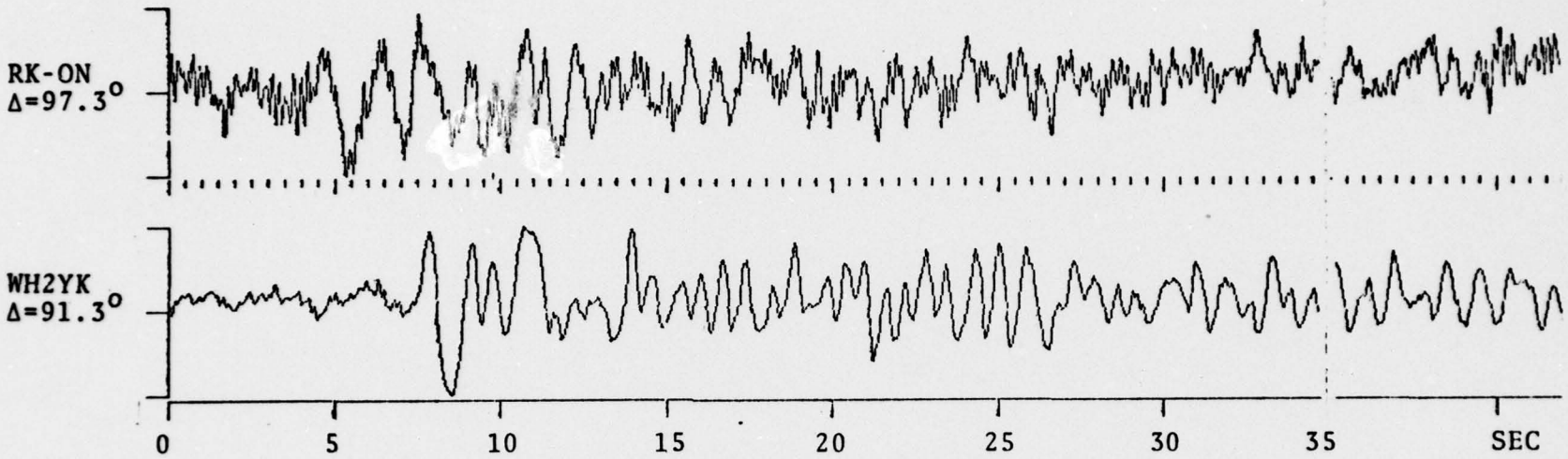

Figure A15

Iran Event (3/7/75) Seismograms

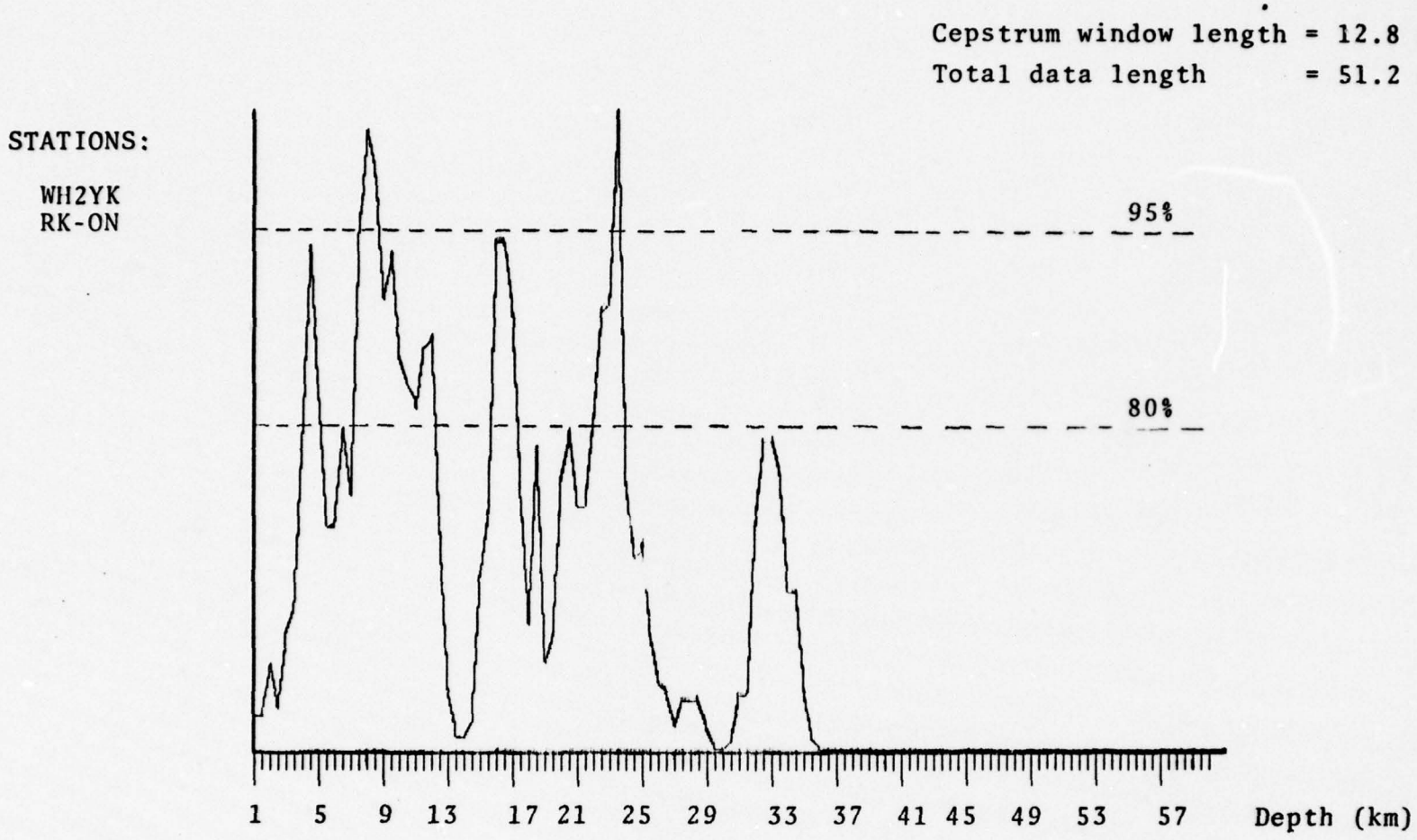

Figure A16

Iran Event (3/7/75), P Depth Plot

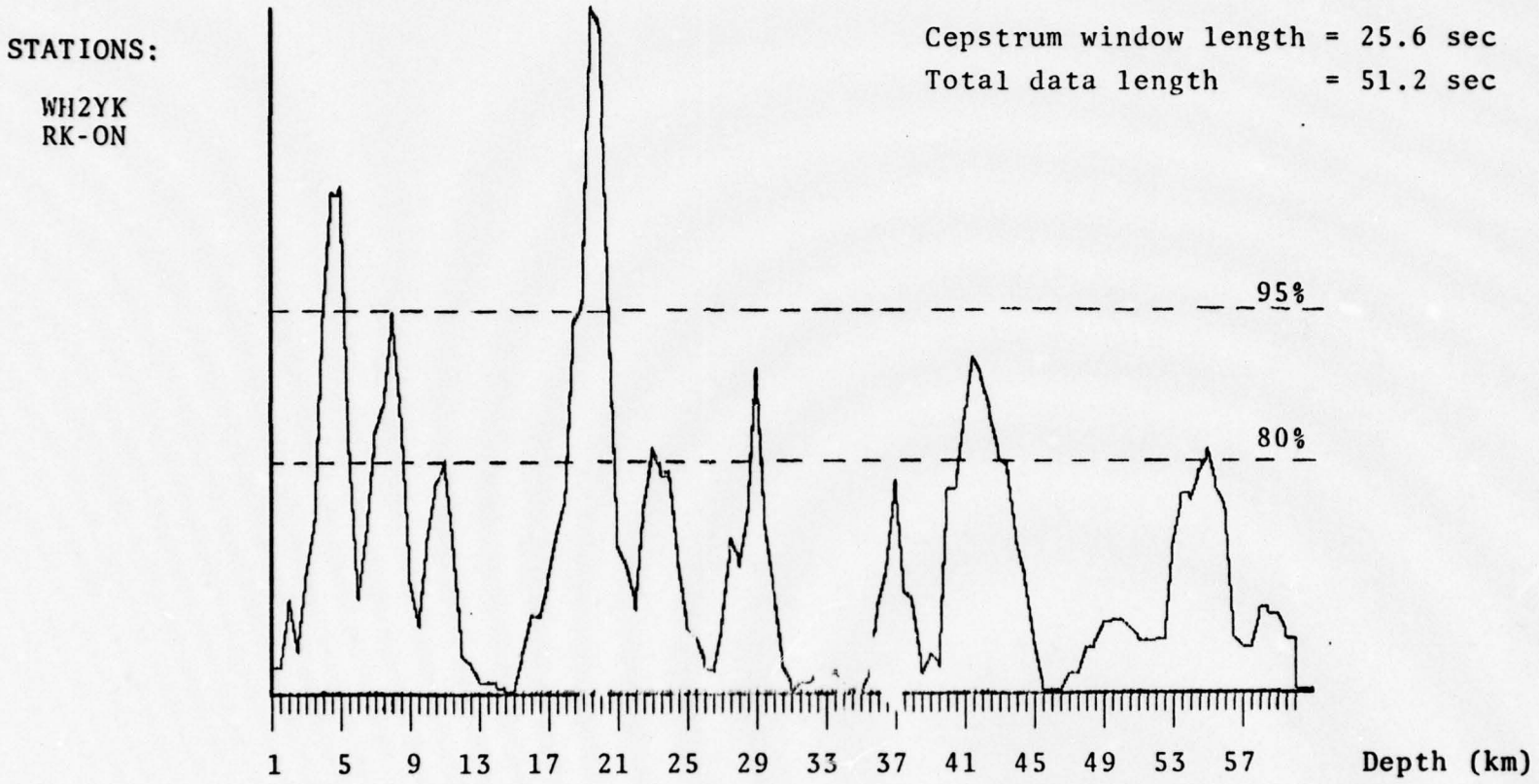

Figure A17

Iran Event (3/7/75), P Depth Plot

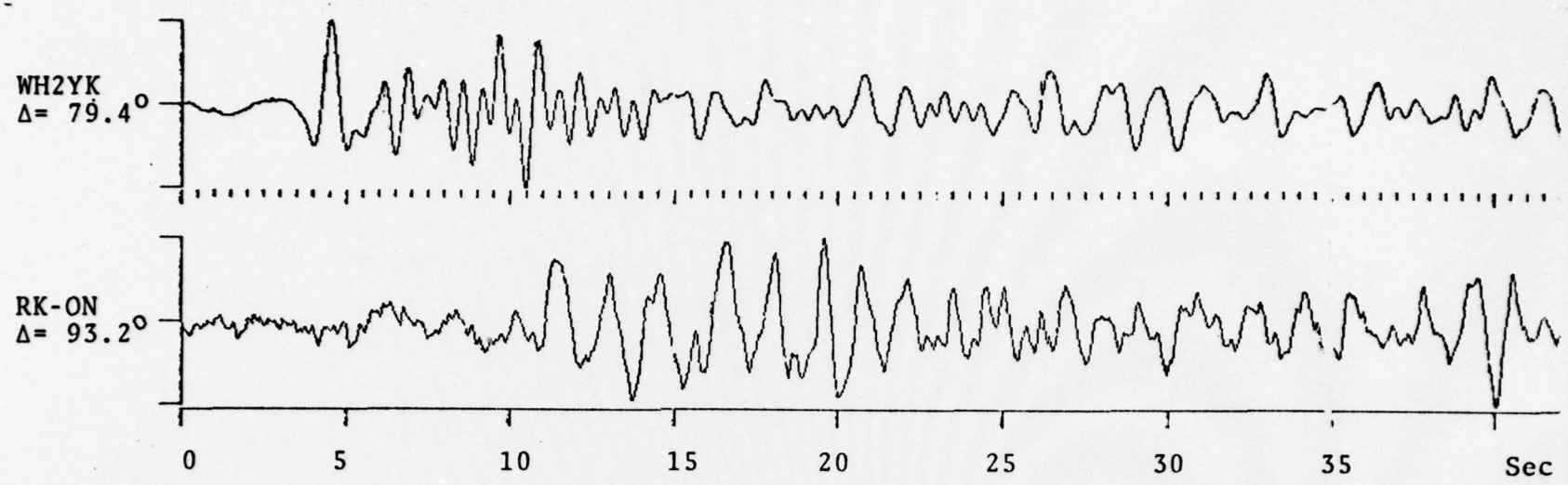

Figure A18

Kasmir Event (4/28/75), Seismograms

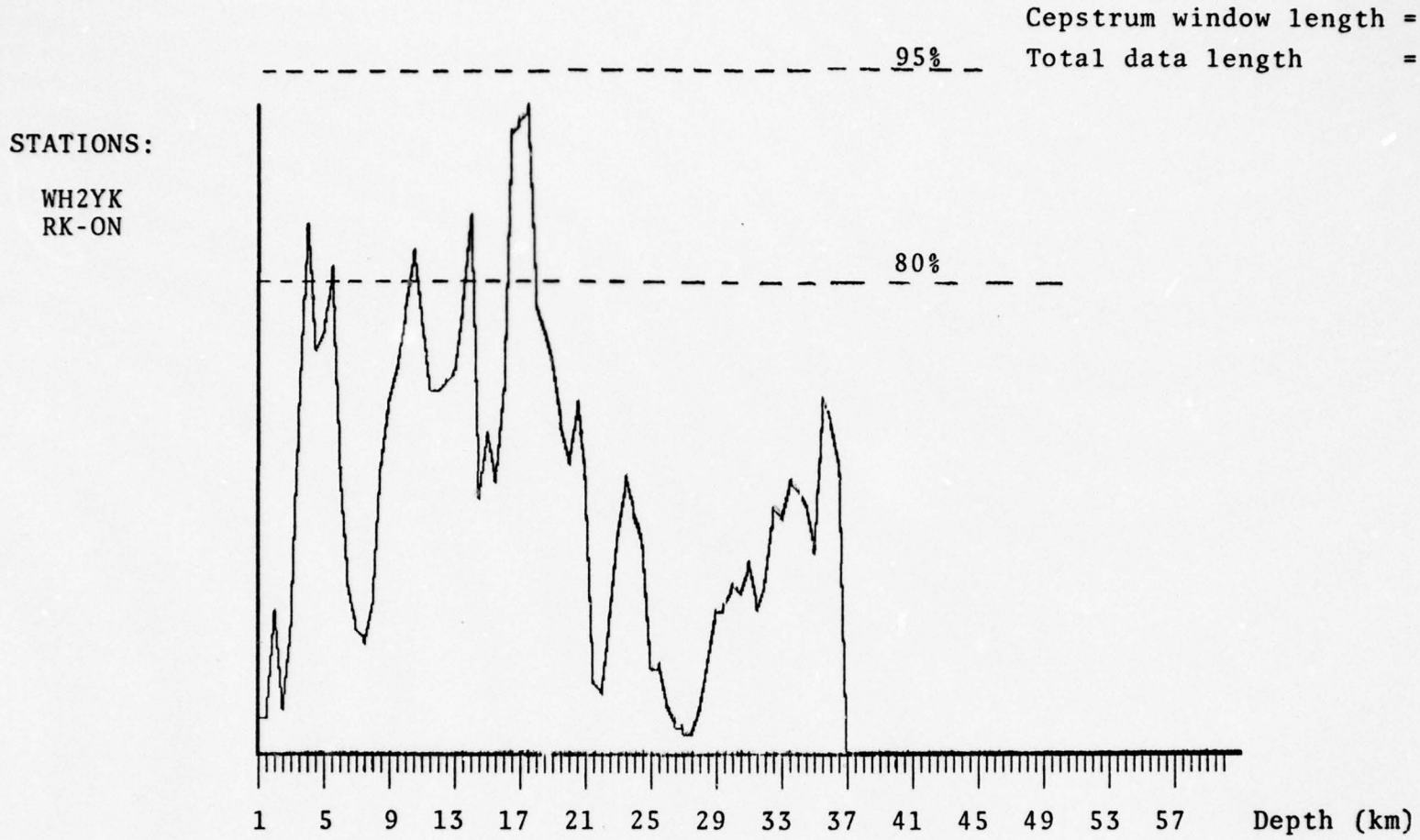

Figure A19

Kasmir Event (4/28/75), P Depth Plot

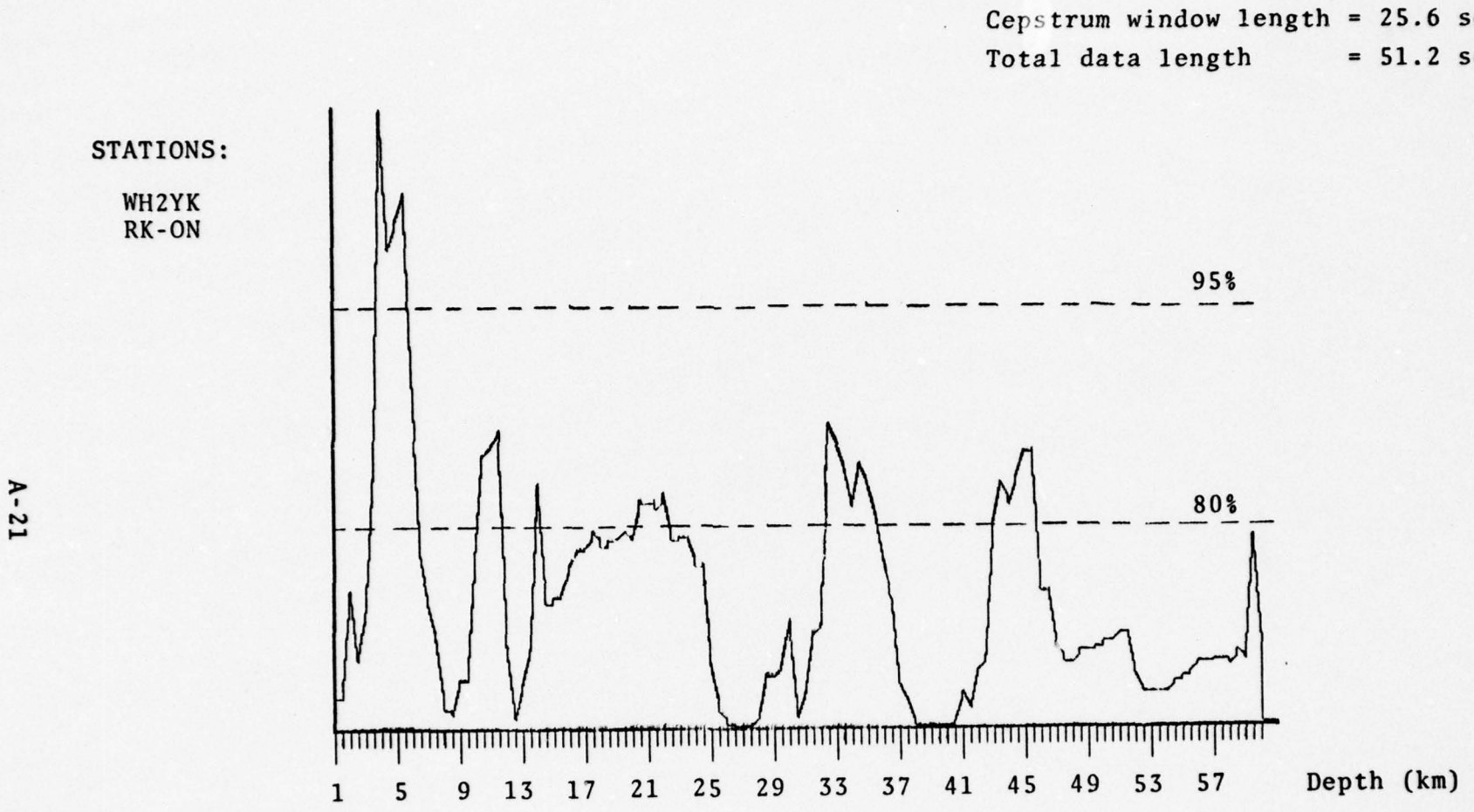

Figure A20

Kasmir Event (4/28/75), P Depth Plot

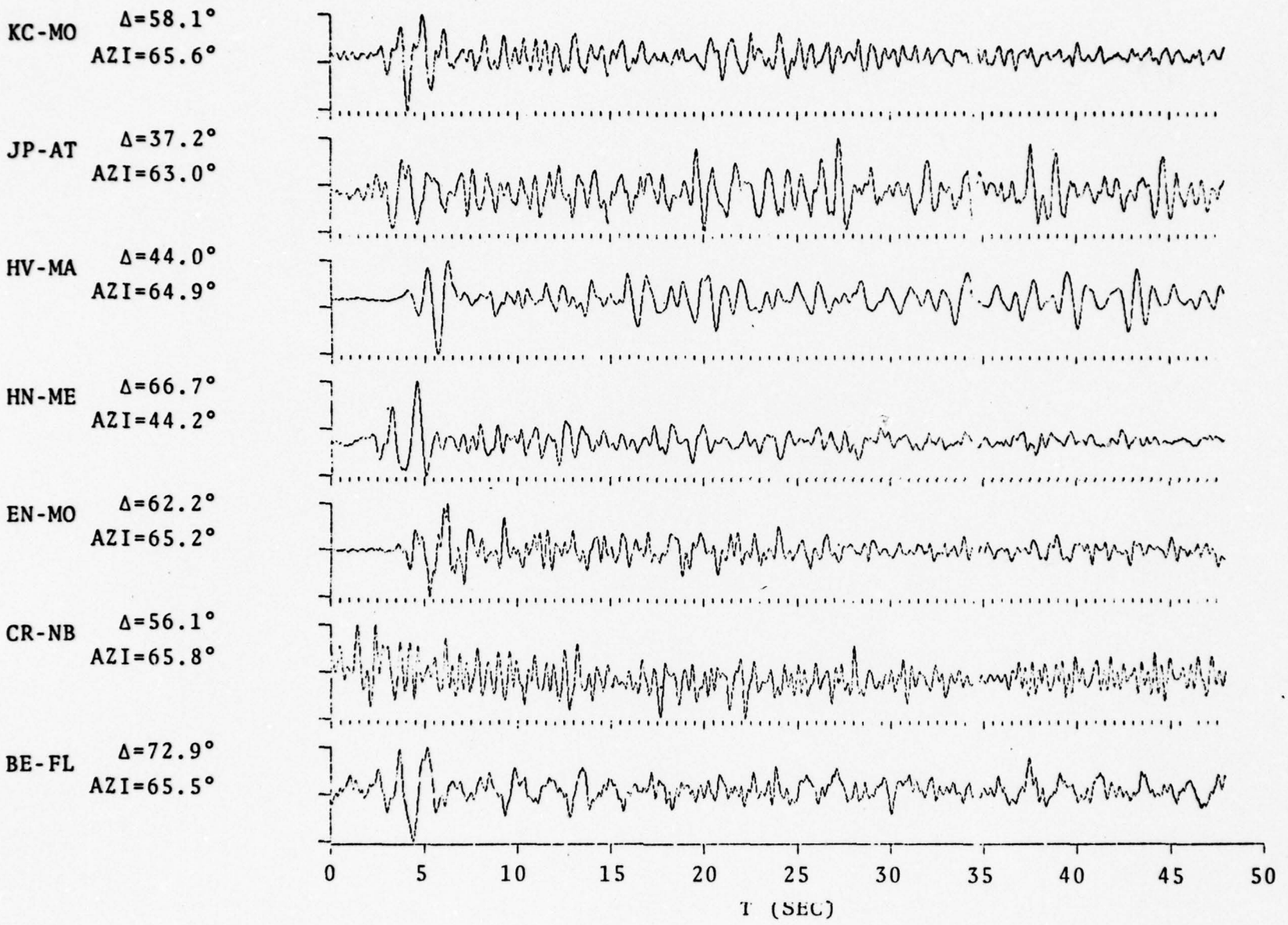

Figure A21

Andreanof Islands Event Seismograms

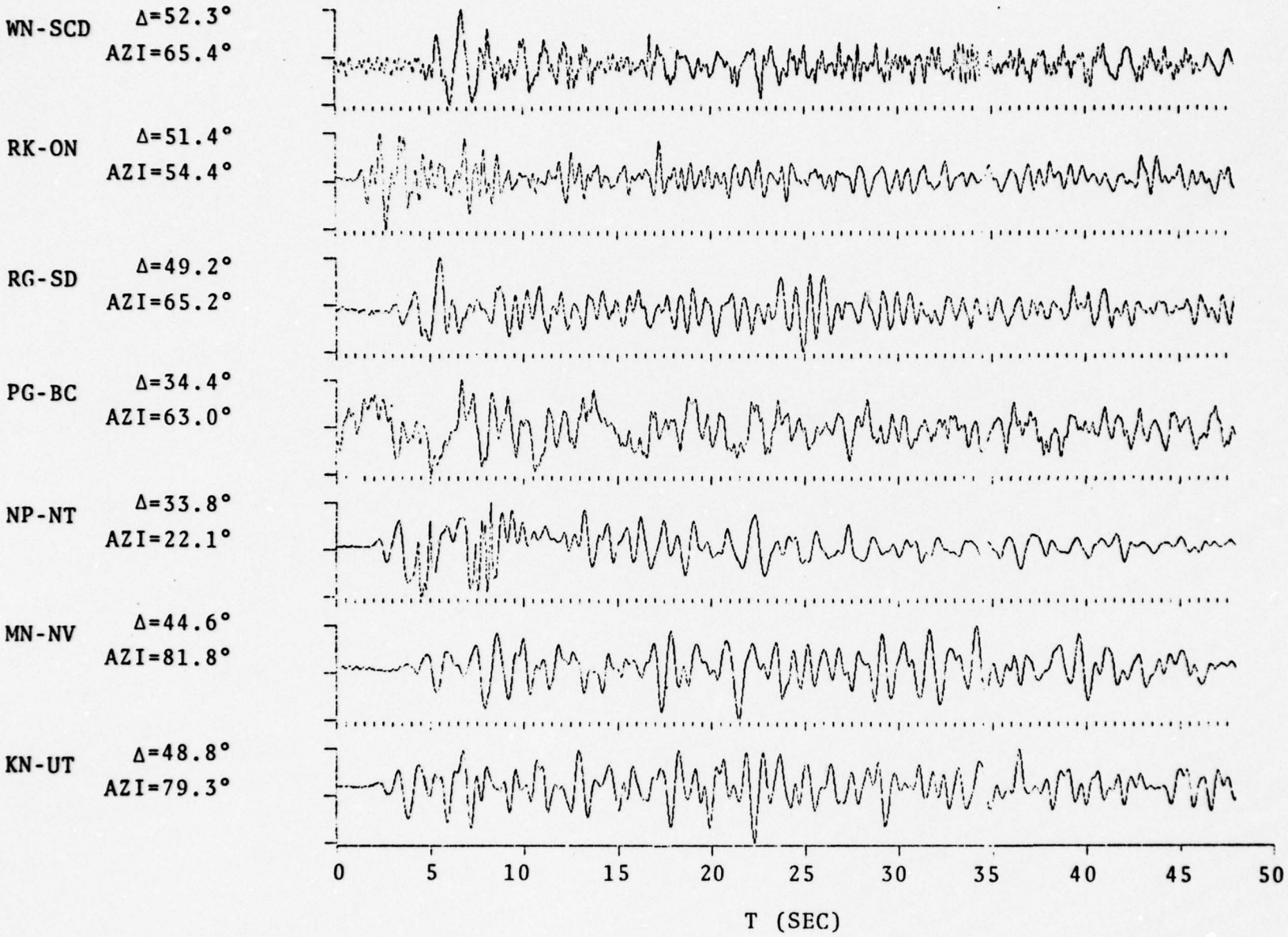

Figure A22

Andreanof Islands Event Seismograms

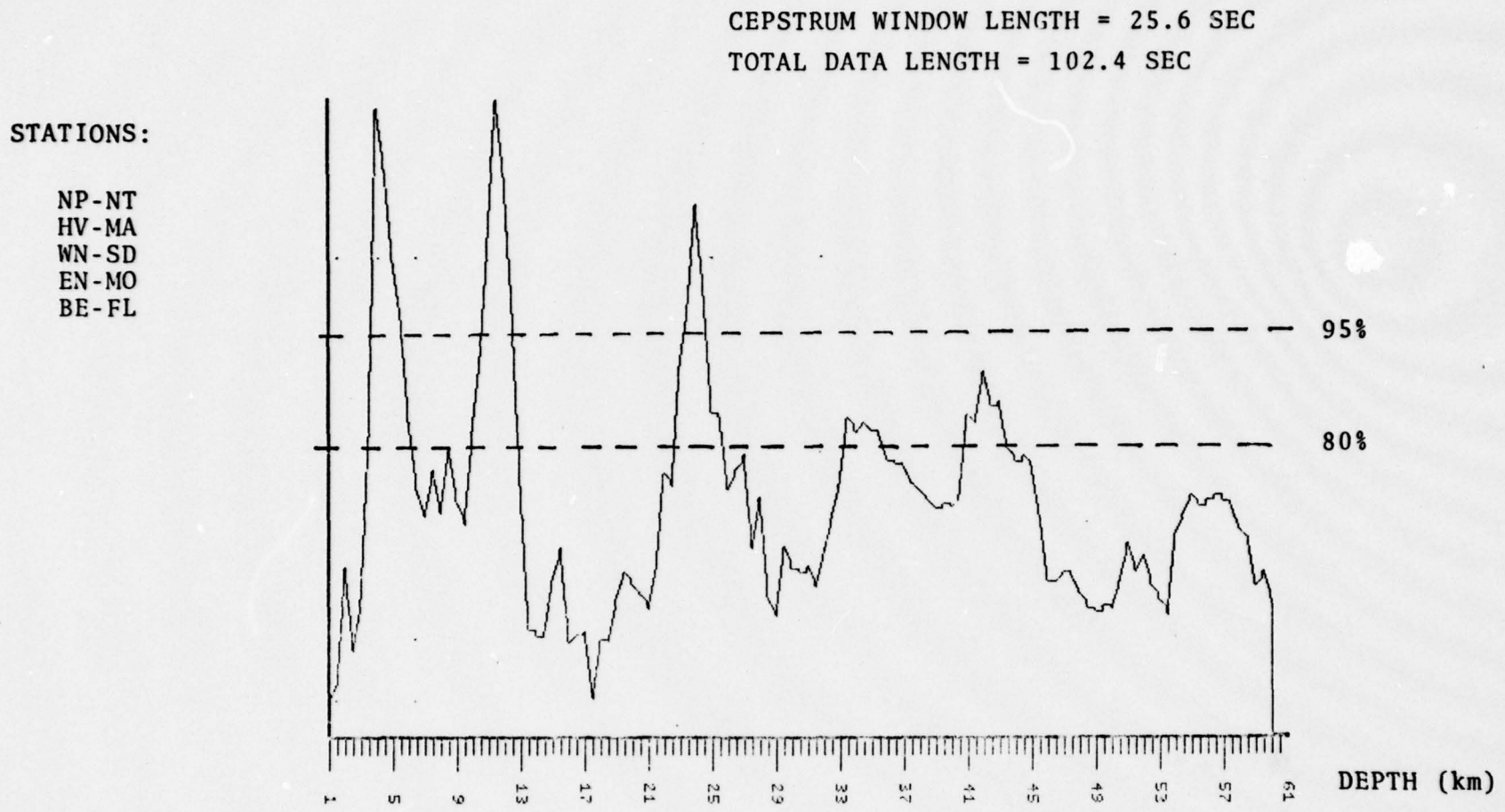

Figure A23

Composite Depth Plot, Data Set 1

Andreanof Islands Event

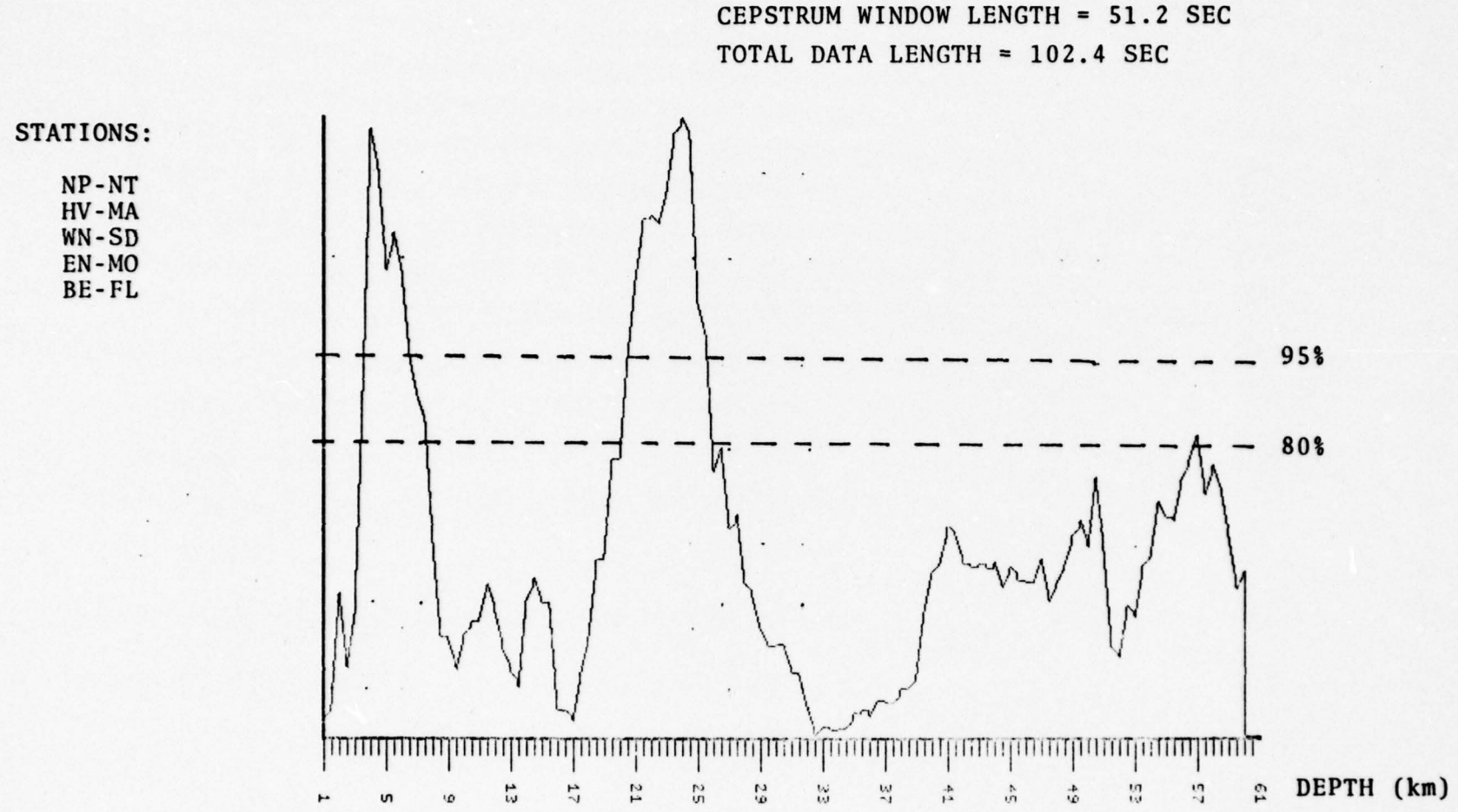

Figure A24

Composite Depth Plot, Data Set 1

Andreanof Islands Event

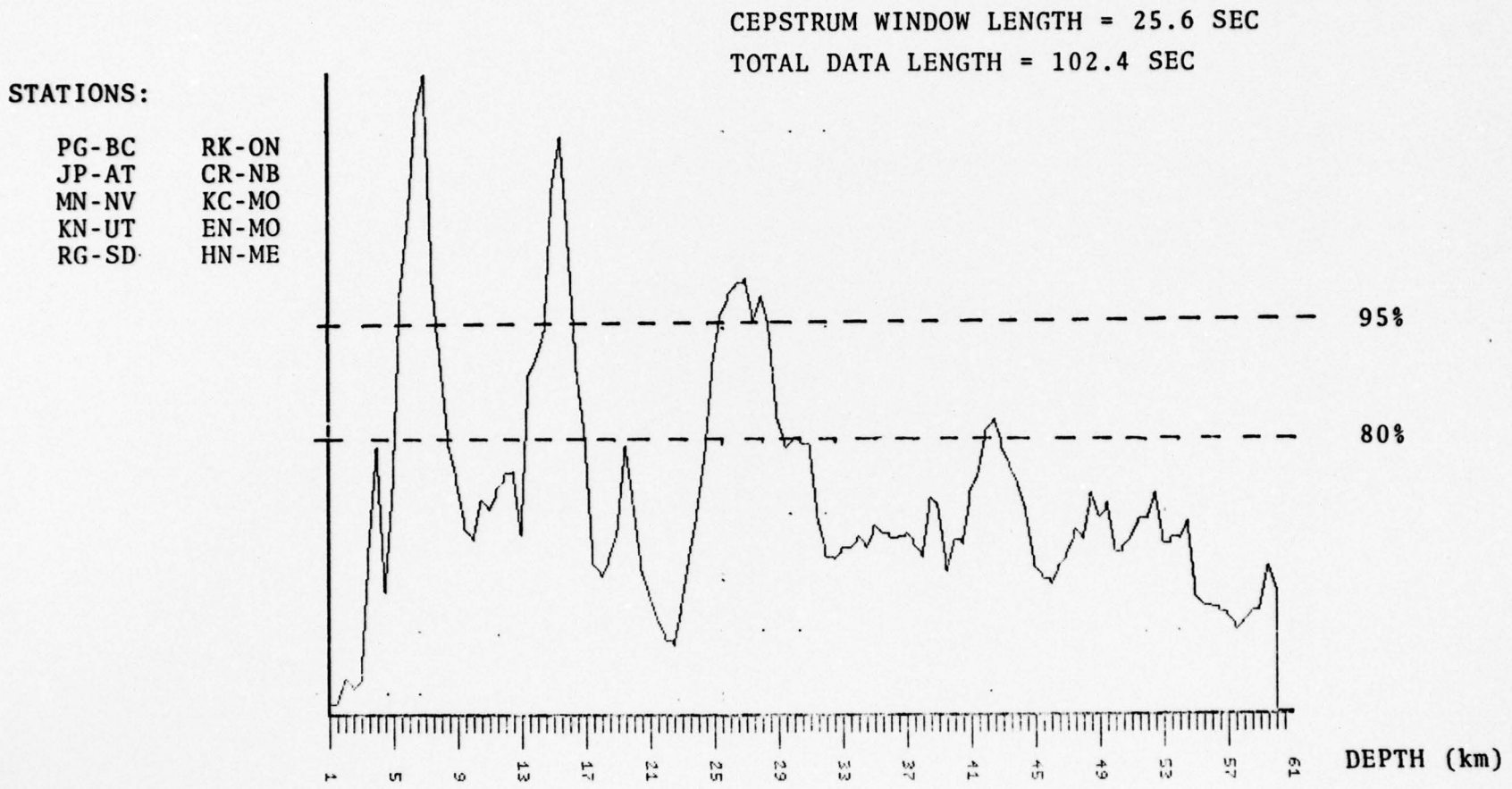

Figure A25

Composite Depth Plot, Data Set 2

Andreanof Islands Event

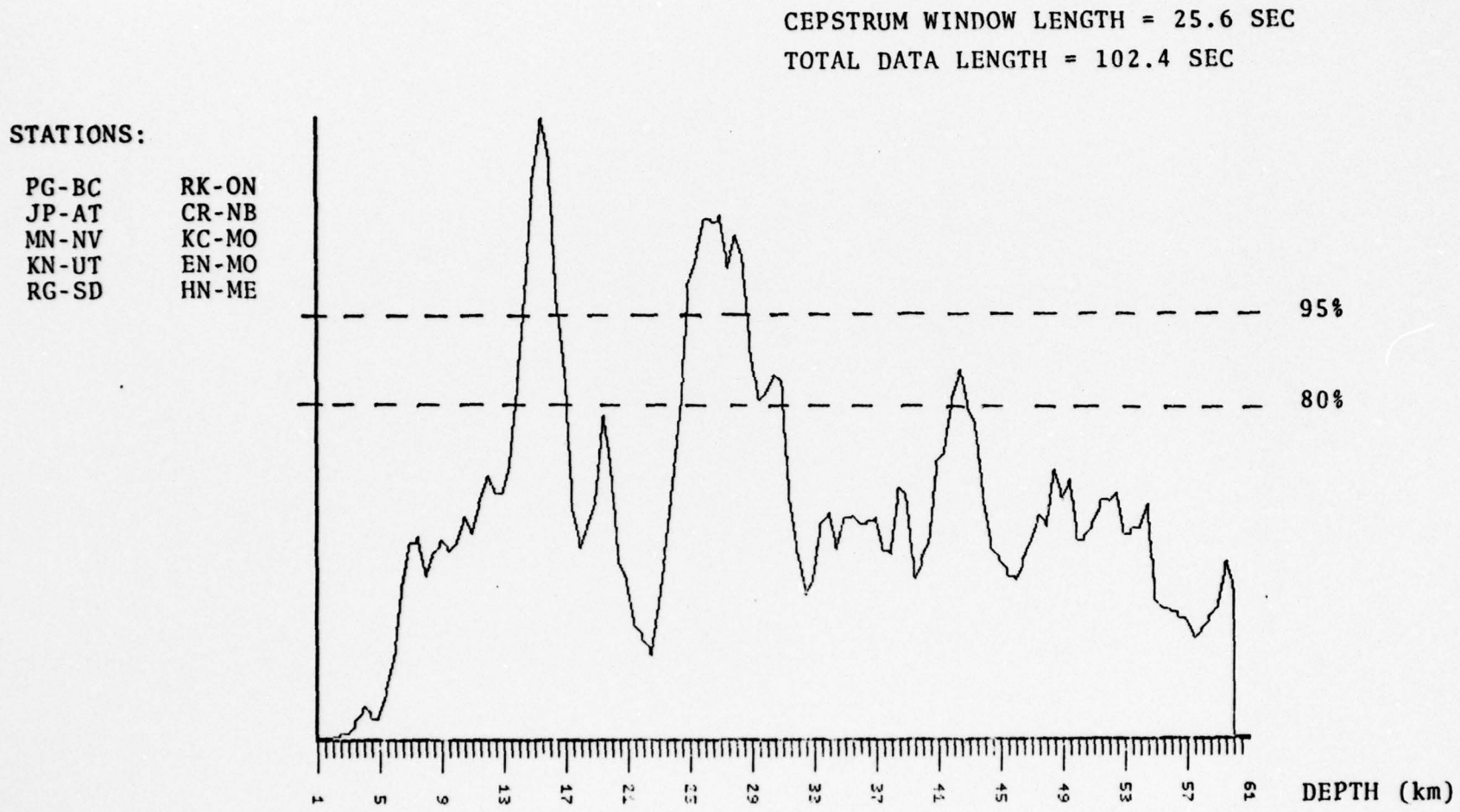

Figure A26
Composite Depth Plot, Data Set 2, Cosine Taper
Andreanof Islands Event

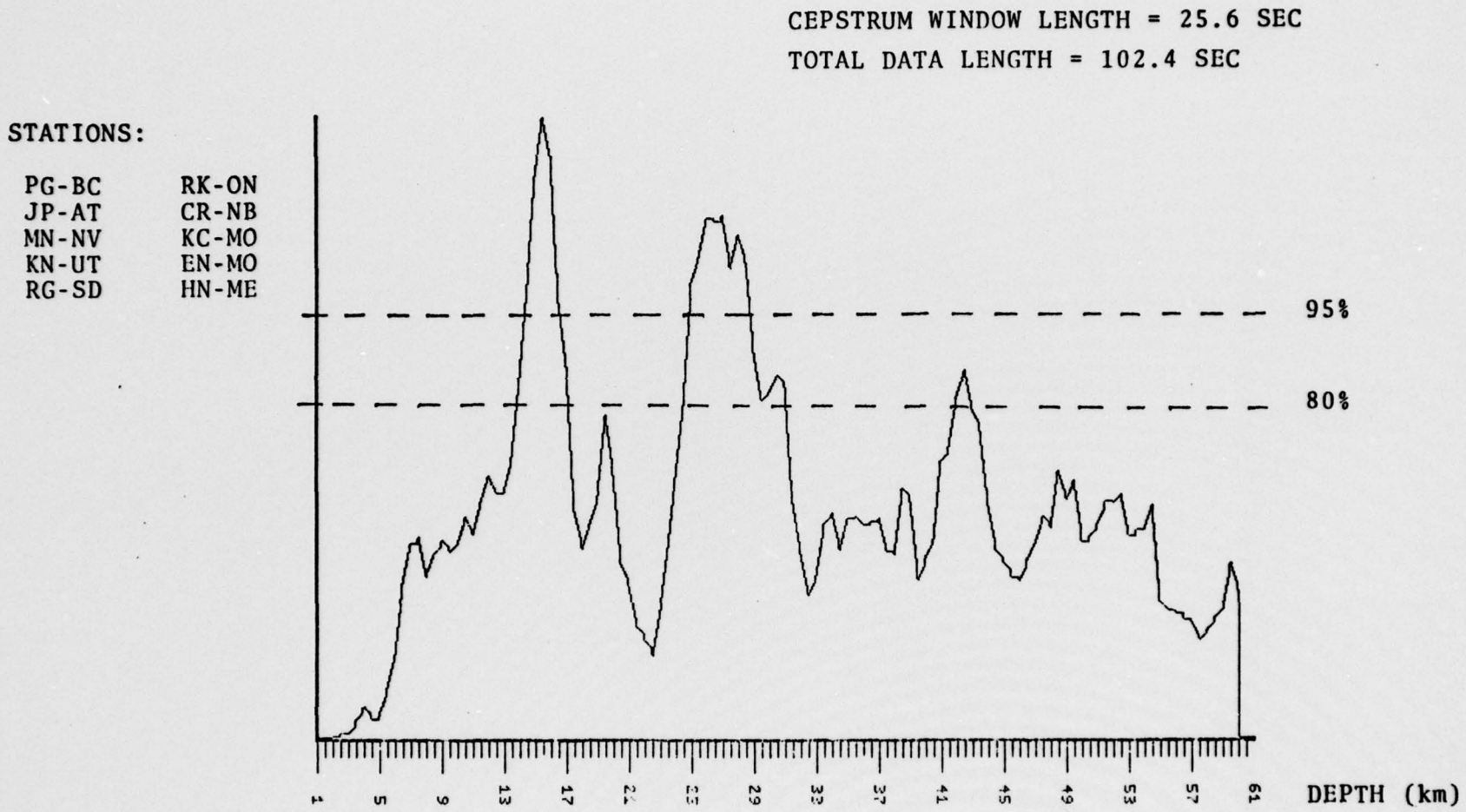

Figure A26
Composite Depth Plot, Data Set 2, Cosine Taper
Andreanof Islands Event

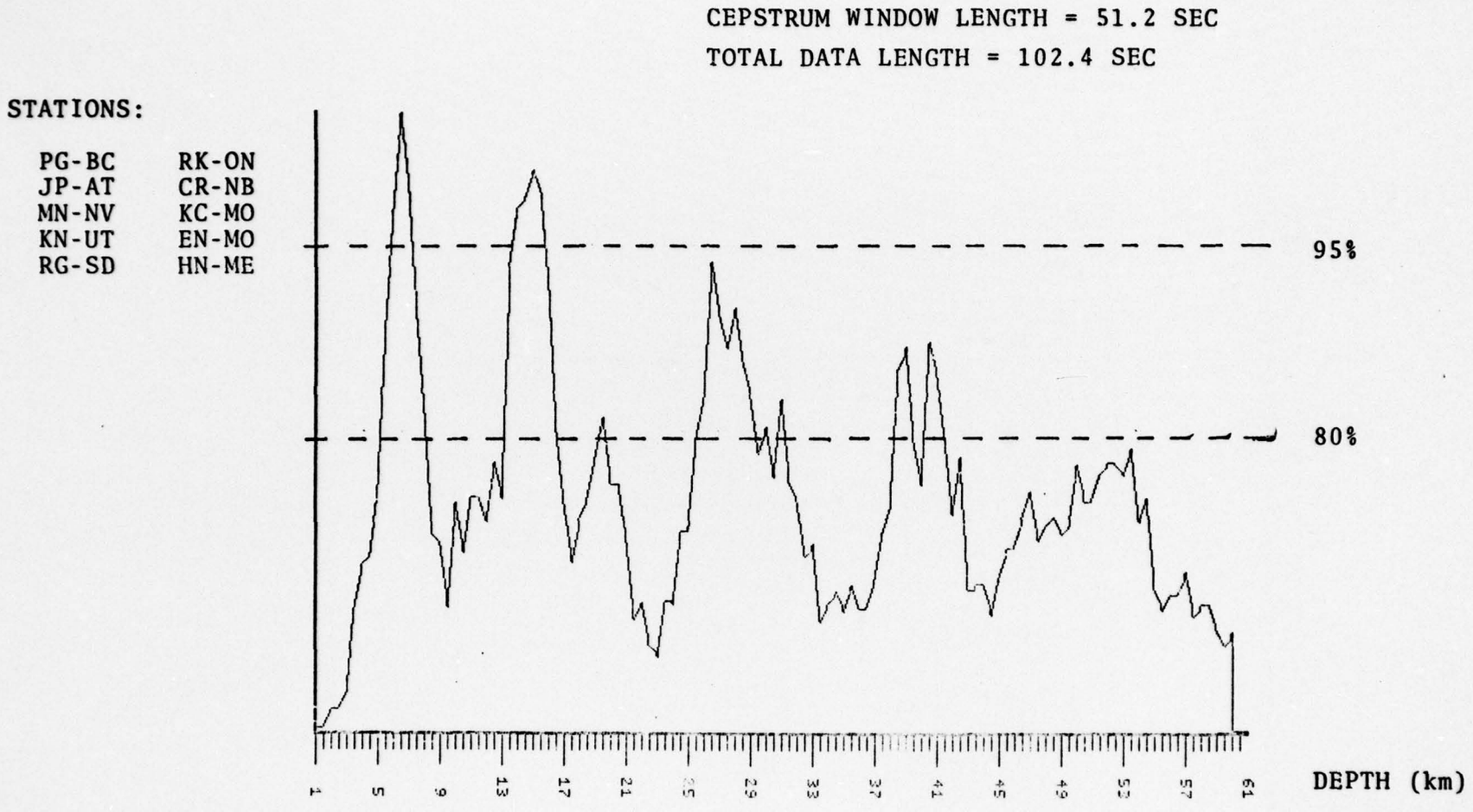

Figure A27

Composite Depth Plot, Data Set 2

Andreanof Islands Event

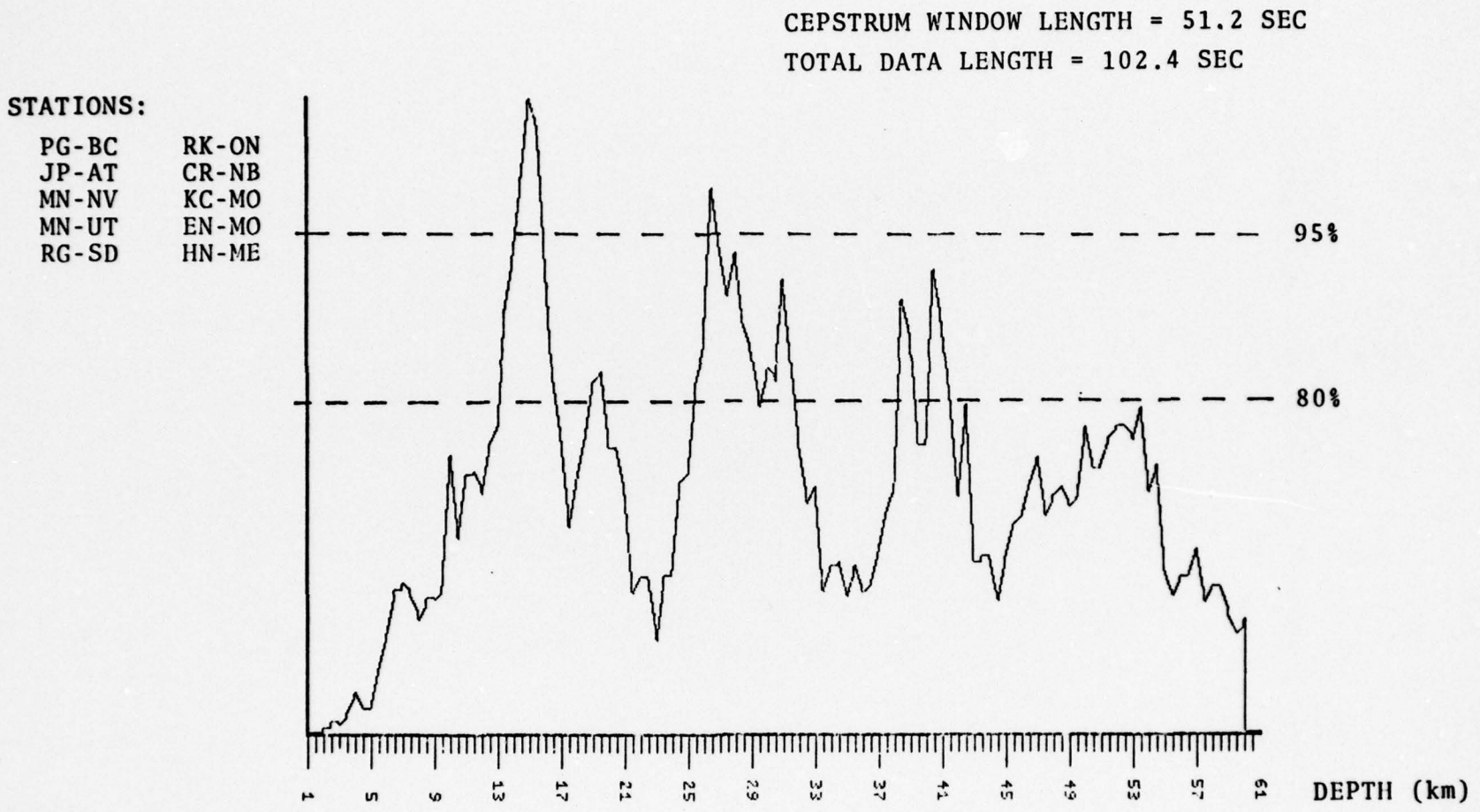

Figure A28

Composite Depth Plot, Data Set 2, Cosine Taper

Andreanof Islands Event

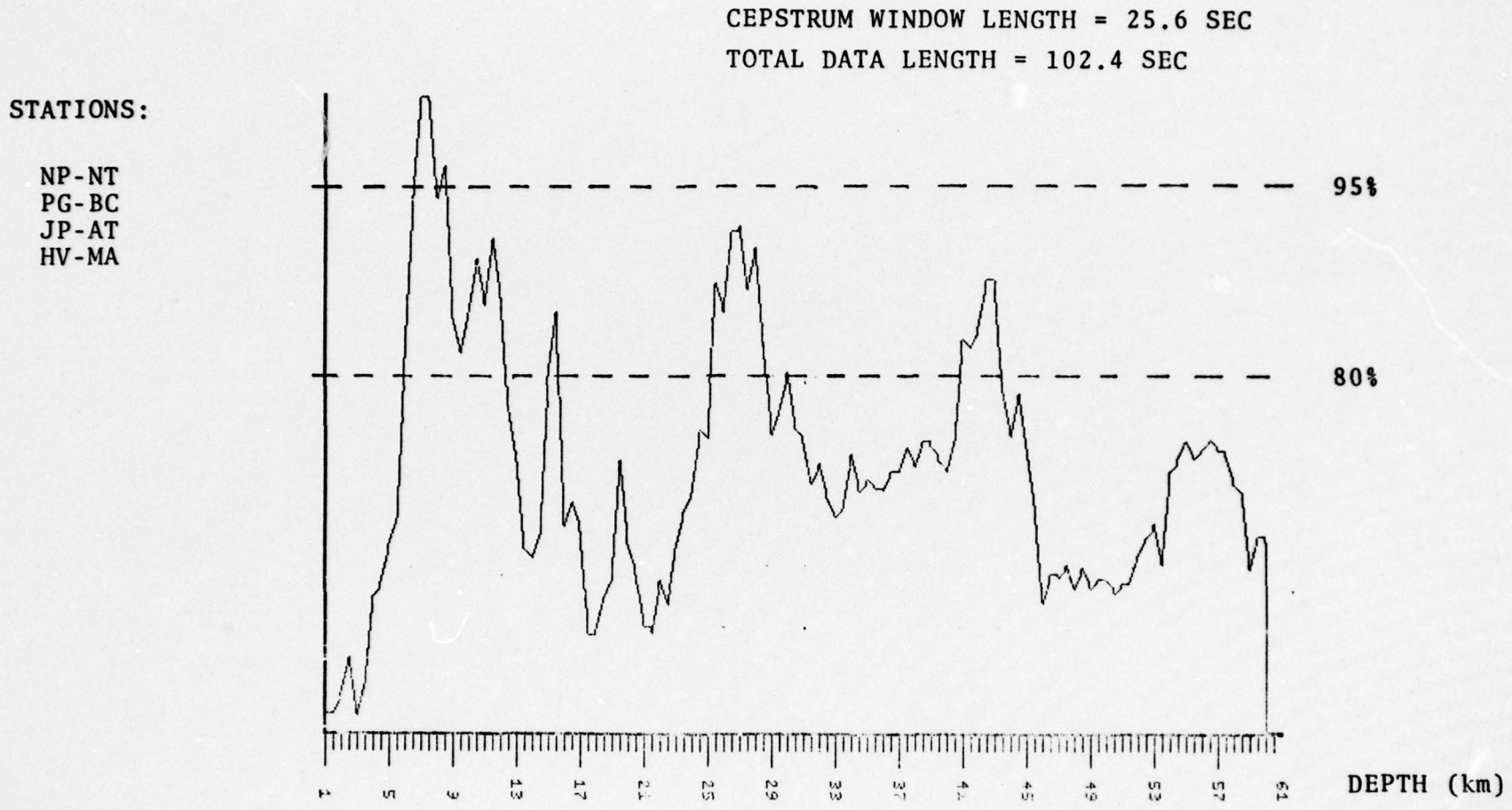

Figure A29

Composite Depth Plot, Data Set 3
Andreanof Islands Event

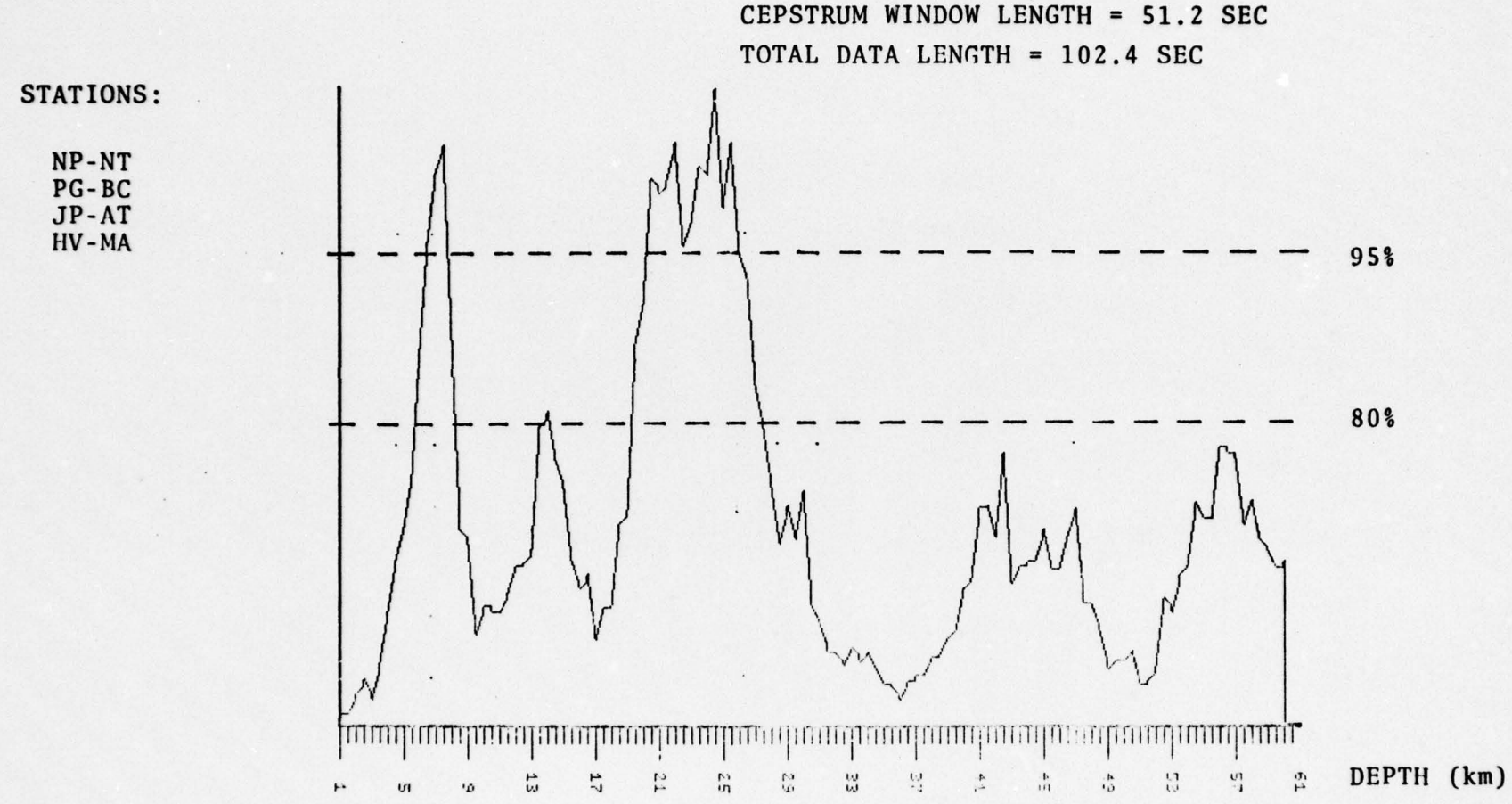

Figure A30

Composite Depth Plot, Data Set 3

Andreanof Islands Event

CEPSTRUM WINDOW LENGTH = 25.6 SEC
TOTAL DATA LENGTH = 102.4 SEC

STATIONS:

HV-MA
MN-NV
KN-UT
RG-SD
RK-ON
WN-SD

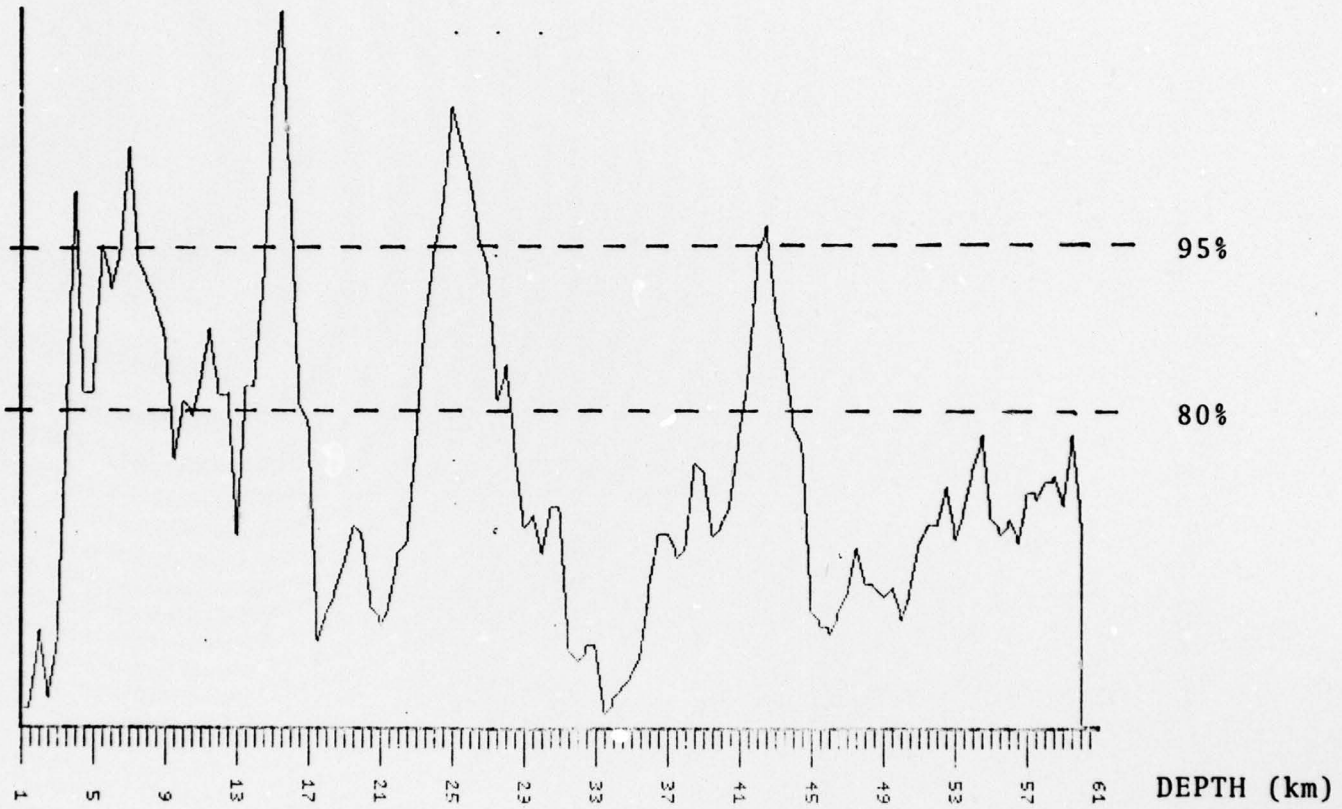

Figure A31

Composite Depth Plot, Data Set 4

Andreanof Islands Event

CEPSTRUM WINDOW LENGTH = 51.2 SEC
TOTAL DATA LENGTH = 102.4 SEC

STATIONS:

HV-MA
MN-NV
KN-UT
RG-SD
RK-ON
WN-SD

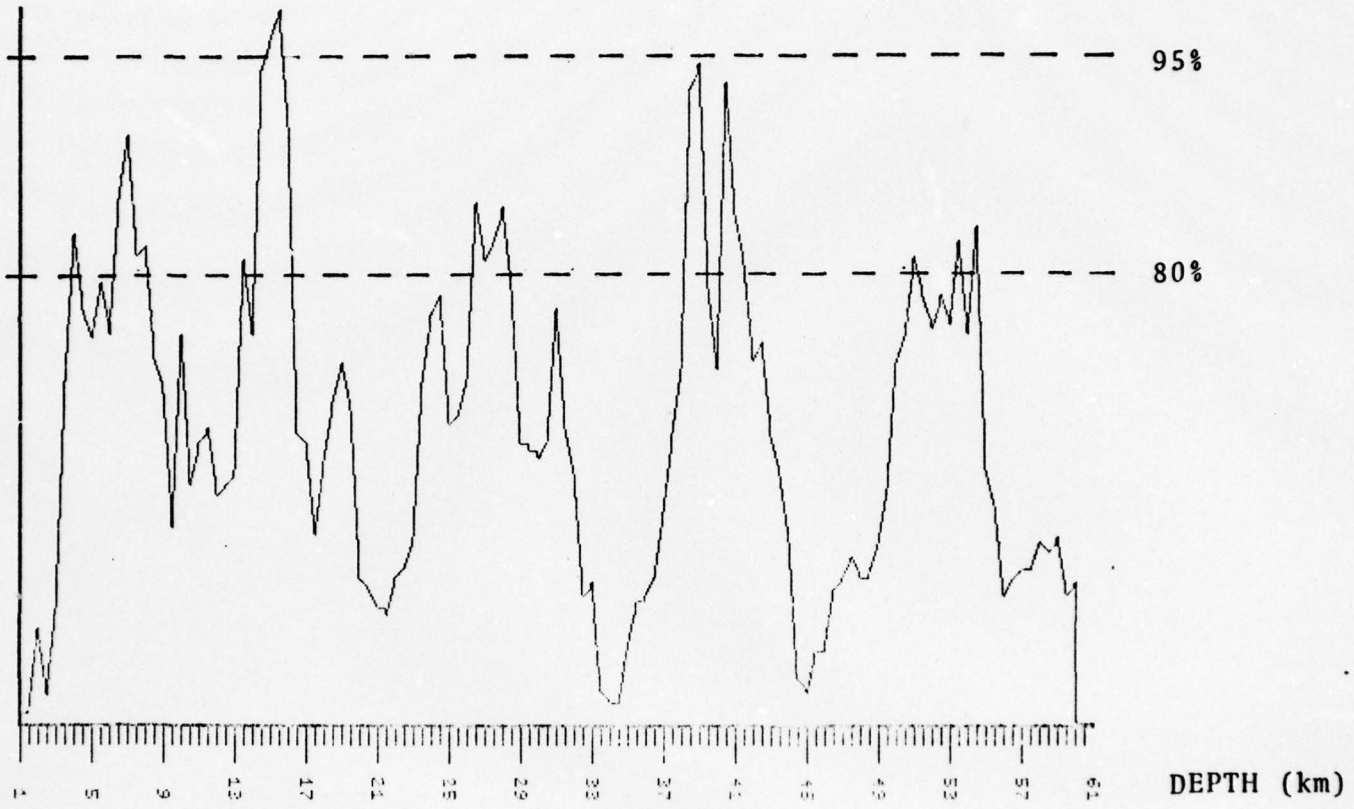

Figure A32

Composite Depth Plot, Data Set 4
Andreanof Islands Event

CEPSTRUM WINDOW LENGTH = 25.6 SEC
TOTAL DATA LENGTH = 102.4 SEC

STATIONS:

CR-NB
KC-MO
EN-MO
HN-ME

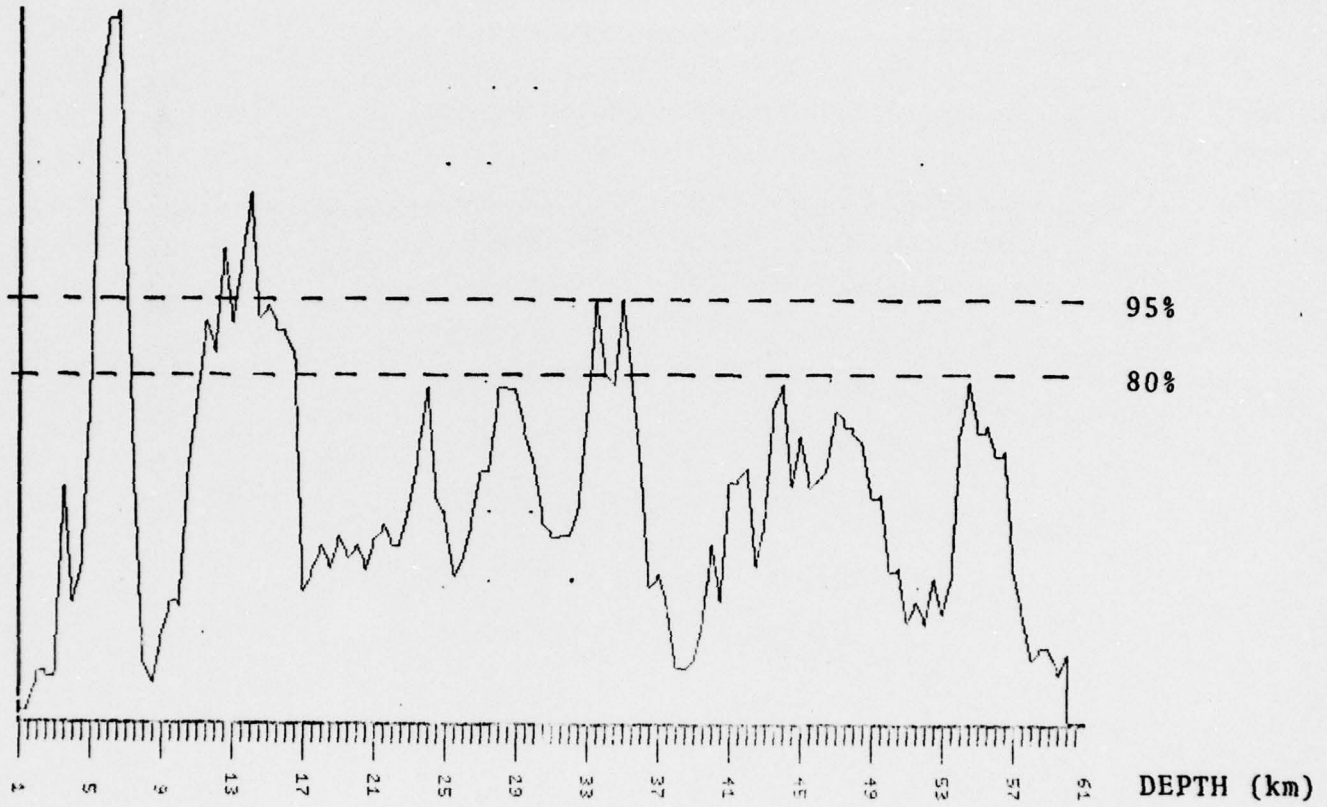

Figure A33

Composite Depth Plot, Data Set 5
Andreanof Islands Event

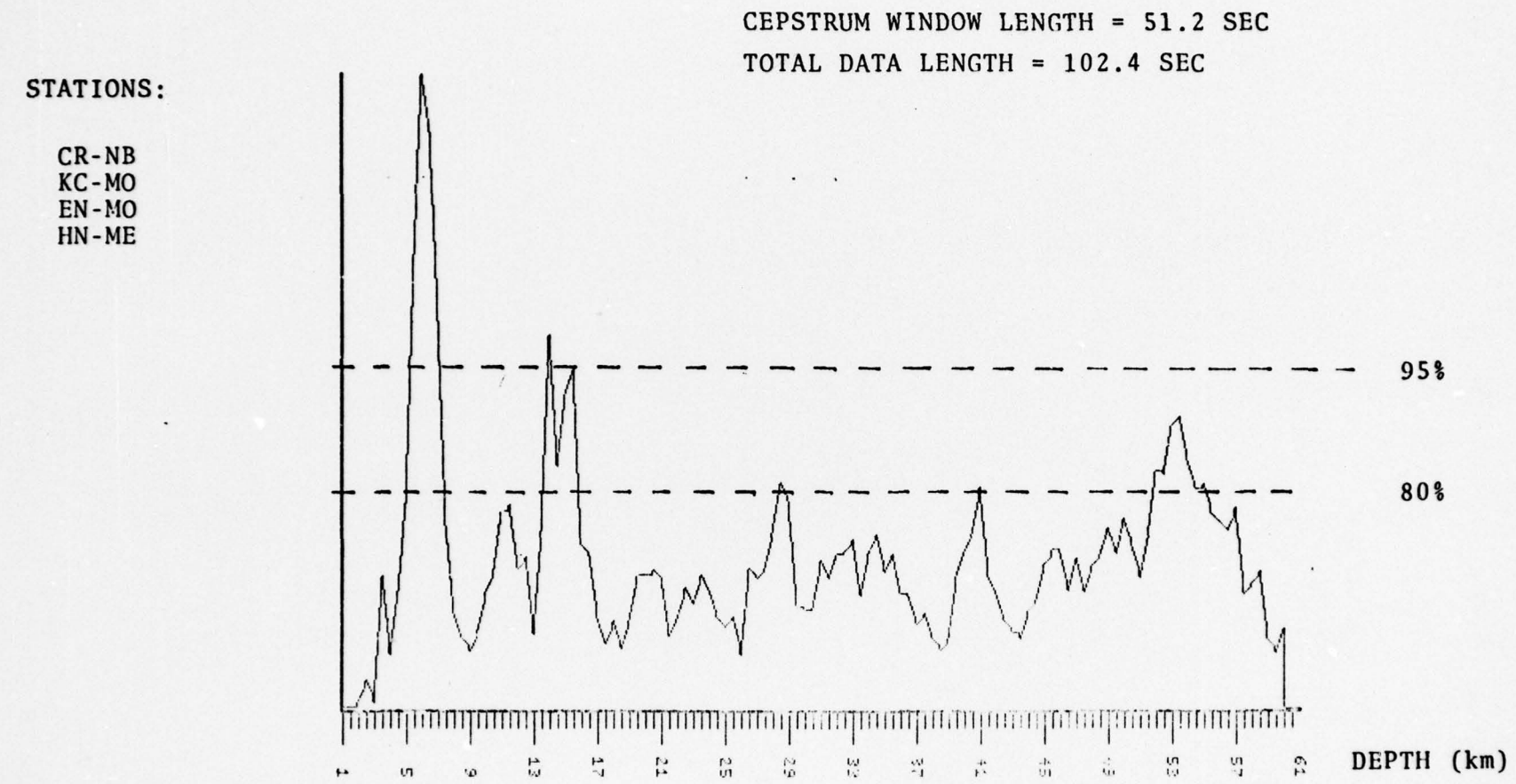

Figure A34

Composite Depth Plot, Data Set 5

Andreanof Islands Event

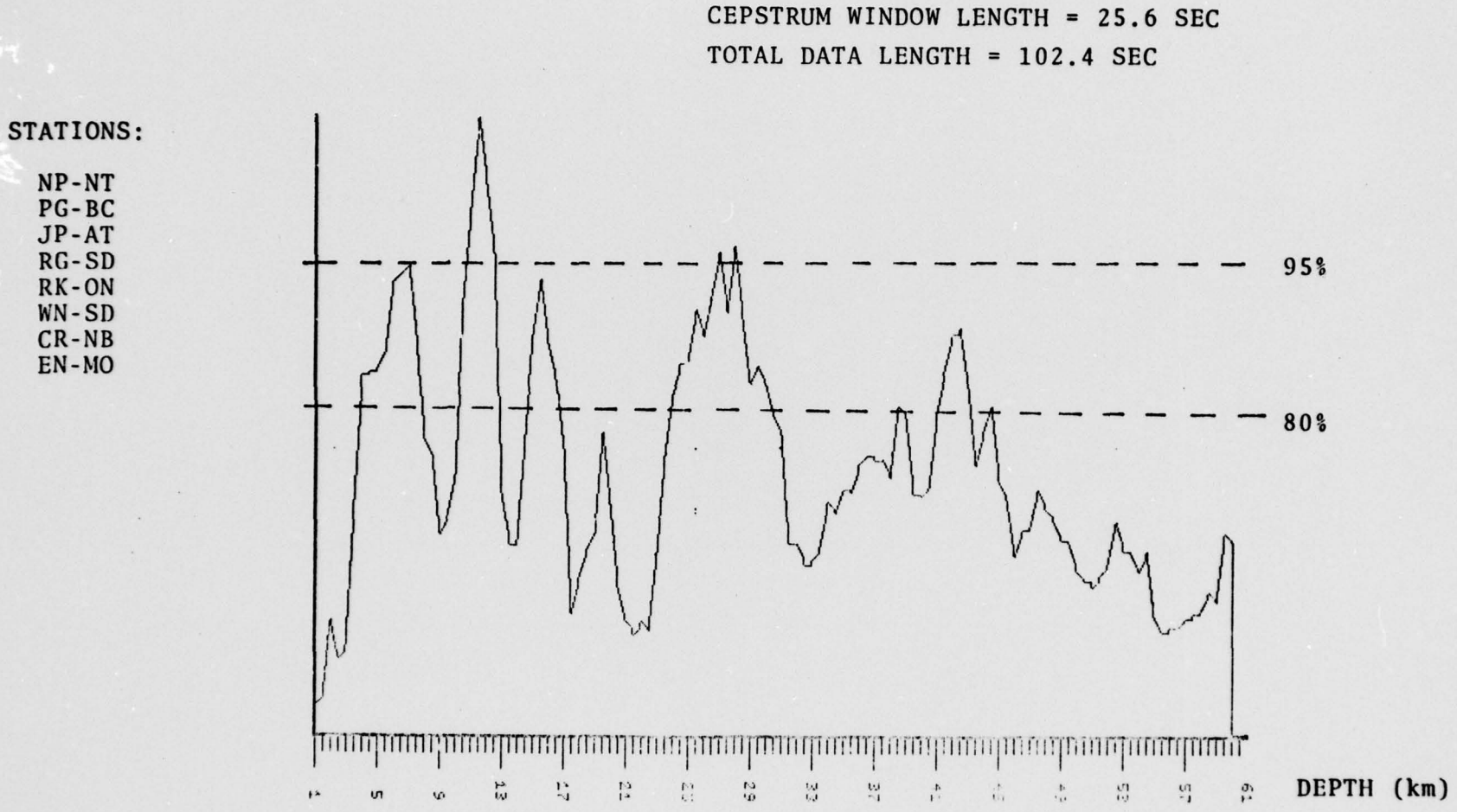

Figure A35

Composite Depth Plot, Data Set 6
Andreanof Islands Event

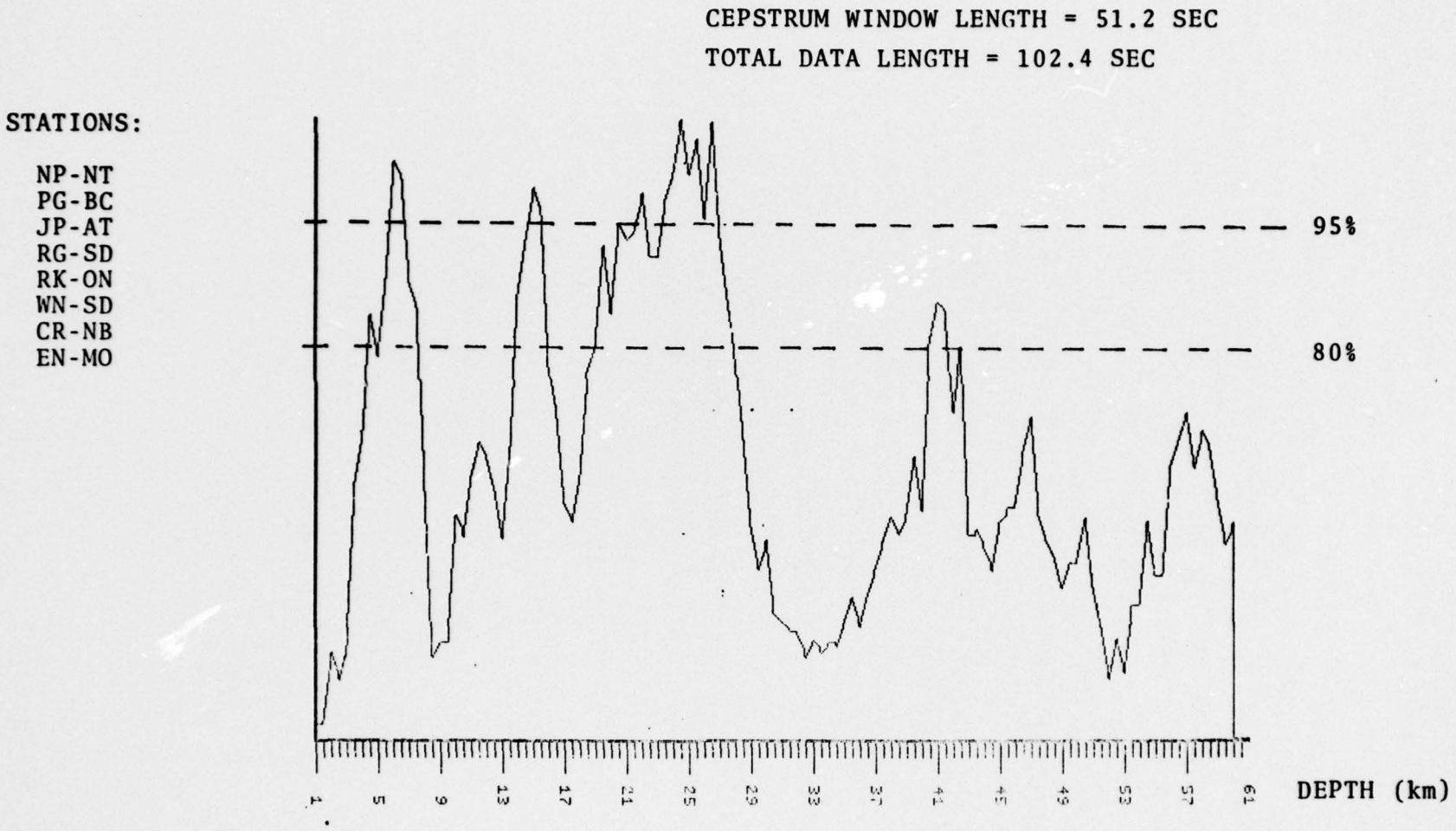

Figure A36

Composite Depth Plot, Data Set 6

Andreanof Islands Event

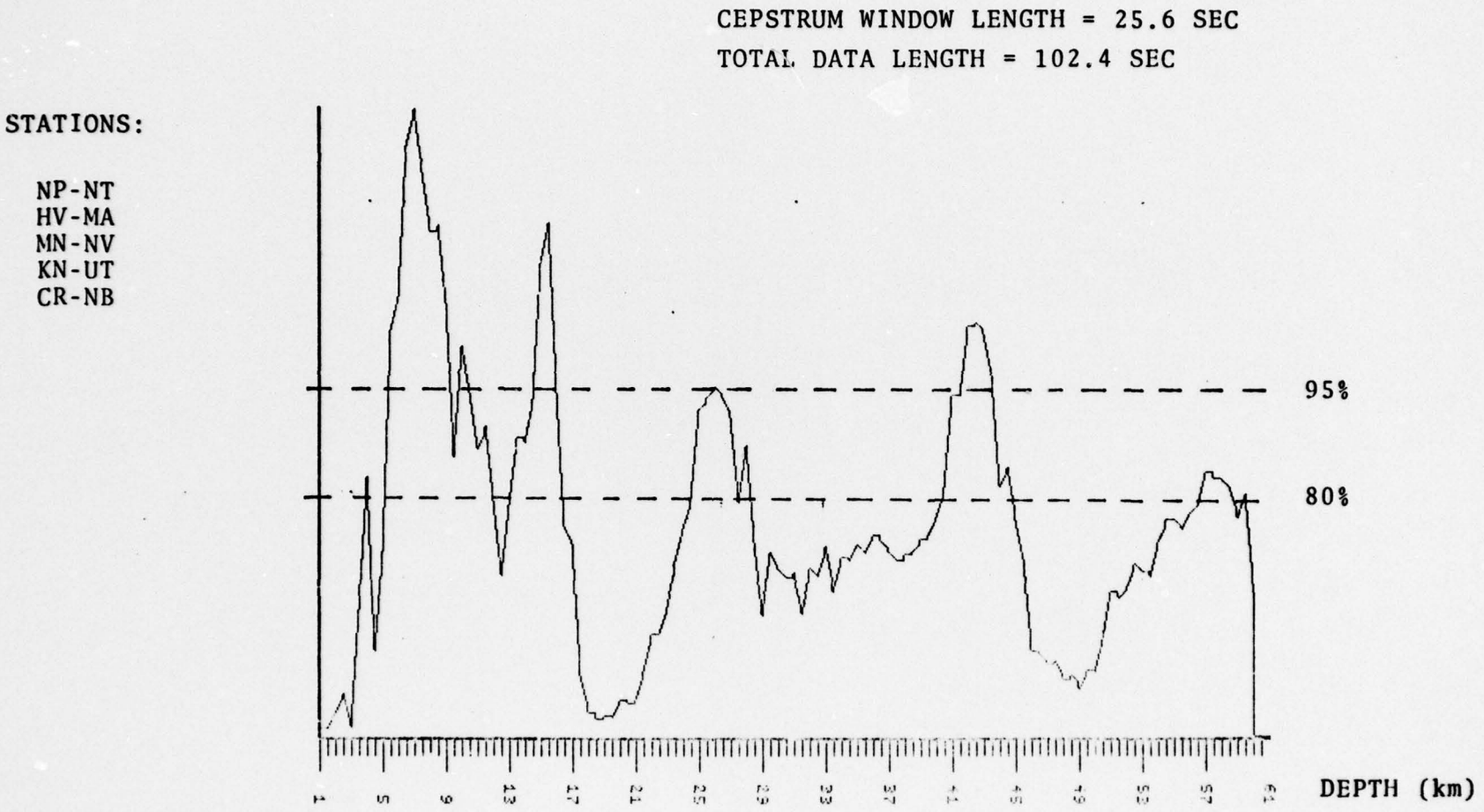

Figure A37

Composite Depth Plot, Data Set 7
Andreanof Islands Event

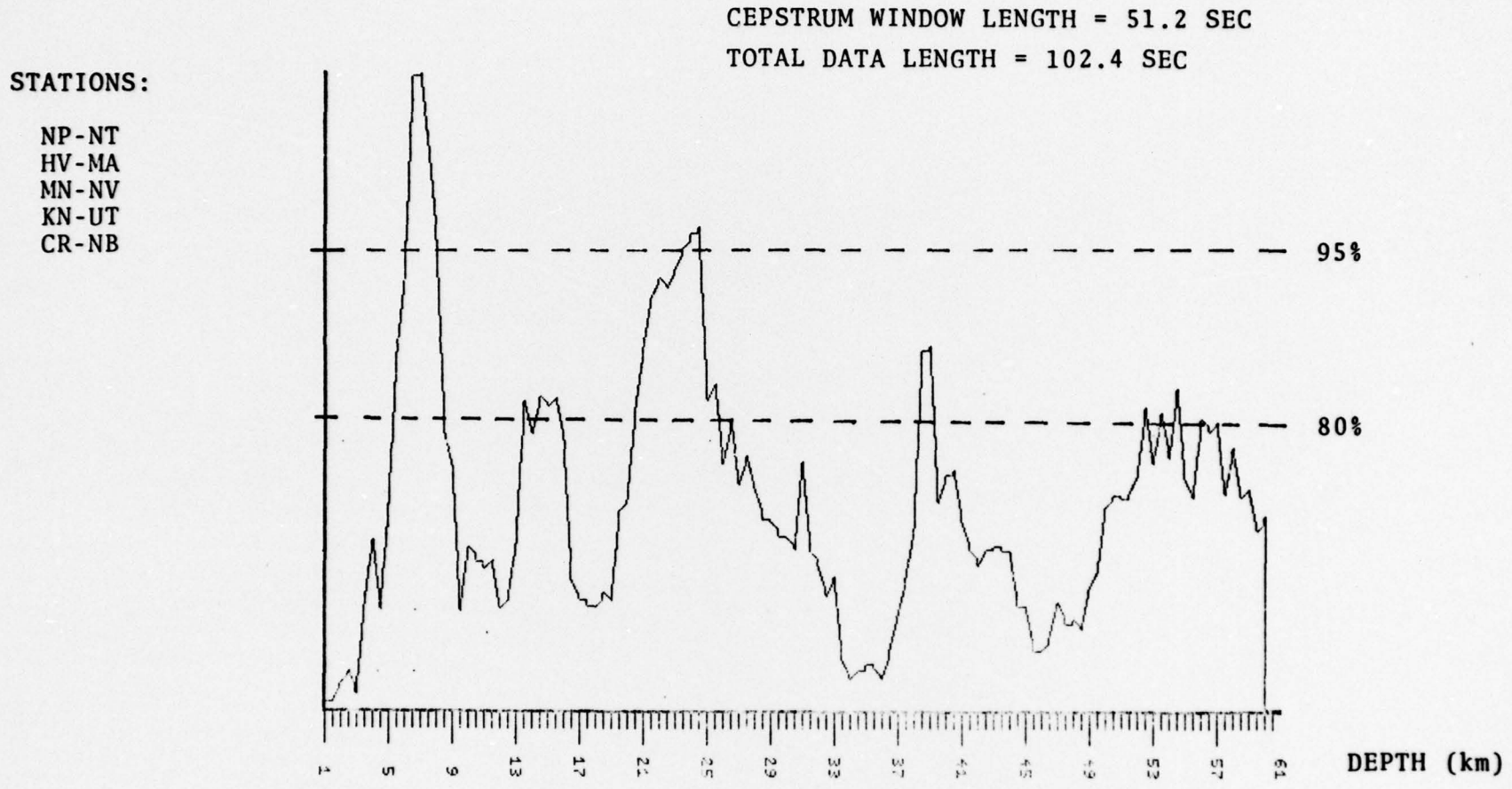

Figure A38

Composite Depth Plot, Data Set 7

Andreanof Islands Event